Journal of Archaeological Science 45 (2014) 284–303

Contents lists available at ScienceDirect

Journal of Archaeological Science

journal homepage: http://www.elsevier.com/locate/jas

Klipdrift Shelter, southern Cape, South Africa: preliminary report on the Howiesons Poort layers

Christopher S. Henshilwood [a,b,*], Karen L. van Niekerk [a], Sarah Wurz [a,b], Anne Delagnes [c,b], Simon J. Armitage [d], Riaan F. Rifkin [a,b], Katja Douze [b], Petro Keene [b], Magnus M. Haaland [a], Jerome Reynard [b], Emmanuel Discamps [a], Samantha S. Mienies [b]

[a] Institute for Archaeology, History, Culture and Religious Studies, University of Bergen, Øysteinsgate 3, N-5007 Bergen, Norway
[b] Evolutionary Studies Institute, University of the Witwatersrand, 1 Jan Smuts Avenue, Braamfontein 2000, Johannesburg, South Africa
[c] Université Bordeaux 1, CNRS UMR 5199 PACEA, Equipe Préhistoire, Paléoenvironnement, Patrimoine, Avenue des Facultés, F-33405 Talence, France
[d] Department of Geography, Royal Holloway, University of London, Egham, Surrey TW20 0EX, UK

ARTICLE INFO

Article history:
Received 23 October 2013
Received in revised form
29 January 2014
Accepted 31 January 2014
Available online 15 February 2014

Keywords:
Middle Stone Age
Howiesons Poort
Homo sapiens
Modern human behaviour
Coastal subsistence
Southern Africa

ABSTRACT

Surveys for archaeological sites in the De Hoop Nature Reserve, southern Cape, South Africa resulted in the discovery of a cave complex comprising two locations, Klipdrift Cave and Klipdrift Shelter. Excavations commenced in 2010 with Later Stone Age deposits initially being recovered at the former site and Middle Stone Age deposits at the latter. The lithic component at Klipdrift Shelter is consistent with the Howiesons Poort, a technological complex recorded at a number of archaeological sites in southern Africa. The age for these deposits at Klipdrift Shelter, obtained by single grain optically stimulated luminescence, spans the period 65.5 ± 4.8 ka to 59.4 ± 4.6 ka. Controlled and accurate excavations of the discrete layers have resulted in the recovery of a hominin molar, marine shells, terrestrial fauna, floral remains, organic materials, hearths, lithics, ochre, and ostrich eggshell. More than 95 pieces of the latter, distributed across the layers, are engraved with diverse, abstract patterns. The preliminary results from Klipdrift Shelter presented in this report provide new insights into the Howiesons Poort in this subregion and contribute further to ongoing knowledge about the complex behaviours of early Homo sapiens in southern Africa. Excavations at the Klipdrift Complex will continue in the future.

1. Introduction

From 1998 to 2009 intermittent archaeological site surveys by two of the authors (CSH and KvN) along 60 km of coastline located in the De Hoop Nature Reserve, southern Cape, South Africa (Fig. 1) resulted in the detailed mapping of more than 160 archaeological sites. In 2010 two of the sites that comprise the Klipdrift Complex, Klipdrift Shelter (KDS) and Klipdrift Cave (KDC), were selected for test excavations (Figs. 1–3). The excavations form a part of the Tracsymbols project, funded by a European Research Council FP7 grant (2010–2015) (http://tracsymbols.eu/), with one key aim being to initiate new excavations at Late Pleistocene archaeological sites in southern Africa. The selection of the Klipdrift sites was based on their visible, *in situ* Later Stone Age (LSA) and Middle Stone Age (MSA) deposits, the preserved fauna and their relative accessibility. In 2011 test excavations commenced at KDS (Figs. 2 and 3) revealing c. 1.6 m deep, well preserved, horizontal MSA deposits immediately below the steeply sloping, eroded surface (Fig. 4c). The clear separation of stratigraphic layers enabled the accurate recovery of materials from discrete depositional layers. The anthropogenic assemblage contained marine shells, terrestrial faunal remains, microfauna, a human tooth, organic materials, ash lenses and hearths, lithic artefacts, ochre and ostrich eggshell. In 2012 we initiated test excavations at a second MSA site within the complex, Klipdrift Cave Lower (KDCL) (Figs. 2 and 3).

Here we report on the preliminary analysis of the materials recovered from the KDS layers dated at 65.5 ± 4.8 ka to 59.4 ± 4.6 ka by single-grain optically stimulated luminescence (OSL) (Fig. 4). The lithics are typical of those attributed to the Howiesons Poort Industry (HP) in southern Africa. The research emanating from this site has the potential of contributing to current debates about the origins of modern human behaviour with a

* Corresponding author. Institute for Archaeology, History, Culture and Religious Studies, University of Bergen, Øysteinsgate 3, N-5007 Bergen, Norway. Tel./fax: +27 21 4656067.
E-mail address: christopher.henshilwood@ahkr.uib.no (C.S. Henshilwood).

http://dx.doi.org/10.1016/j.jas.2014.01.033
0305-4403

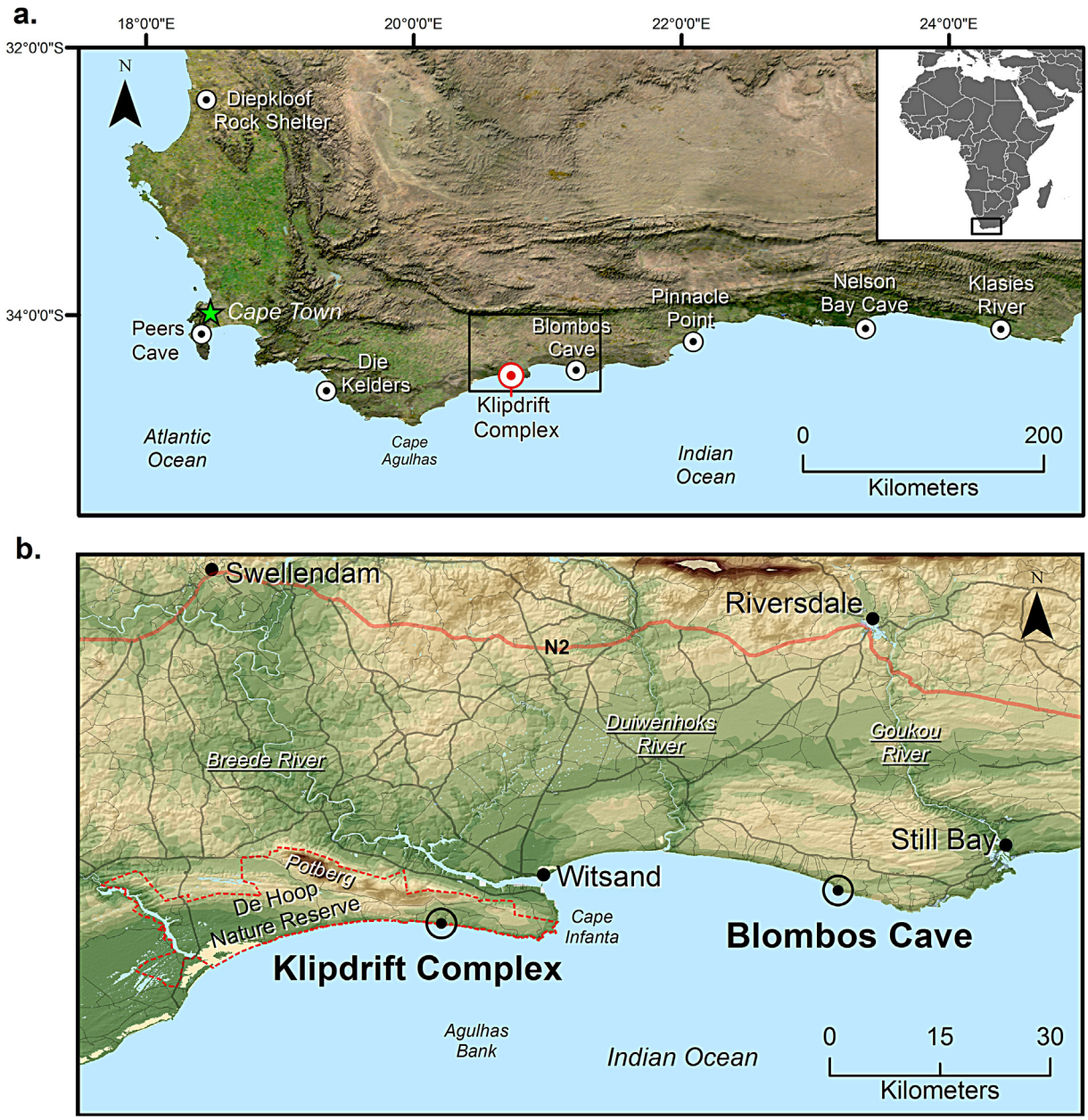

Fig. 1. Location of Klipdrift Complex and sites mentioned in the text.

specific focus on the *Homo sapiens* that inhabited the southern Cape during the MSA. Excavations at KDS and at other sites within the complex will continue in the future.

1.1. Site background

Evidence for human occupation of the De Hoop area from the Acheulean is confirmed by handaxes found near Potberg (Fig. 1) and the numerous LSA and fewer MSA sites distributed mainly along the coast. The Klipdrift Complex is a major depository for Late and Terminal Pleistocene sediments and archaeological deposits that are visible both on the surface and in eroded sections. The Complex is one of several caverns and overhangs along the southern Cape coast formed within the 500–440 Million year (Ma) Table Mountain Group (TMG) sandstones (Deacon and Geleijnse, 1988). Movement along the shear zones within the TMG forms fault breccias susceptible to erosion by high sea levels leading to the formation of caves within the near coastal cliffs (Pickering et al., 2013). KDC and KDS are formed in the TMG sandstones, presumably as a result of this process. In the eastern section of De Hoop, 5 Ma hard dune ridges of Bredasdorp Group limestone infill these TMG shear zones. The seaward extension of the limestone has been truncated by marine erosion and in these coastal cliffs a number of vadose caves have developed above the contact with the TMG (Marker and Craven, 2002).

The Klipdrift Complex (34° 27.0963′S, 20° 43.4582′E), is located in coastal cliffs 12–15 m from the Indian Ocean and c. 19 m above sea level. The larger western cave is c. 21 m deep and contains at least two sites, KDC and KDCL. KDS is a c. 7 m deep shelter, separated from KDC and KDCL by a quartzite promontory (Figs. 2–4). The complex is

Fig. 2. Klipdrift Cave and Klipdrift Shelter towards the north (upper) and west (lower).

located within the eastern section of the De Hoop Nature Reserve (Fig. 1b) on Portion 20 of farm 516, Swellendam district in the Overberg region of the southern Cape. Cape Town is c. 150 km to the west; the *Klipdriftfonteinspruit* stream (namesake of the cave complex) and Noetsie waterfall (Scott and Burgers, 1993), which are perennial sources of fresh water, lie about 200 m east of the Klipdrift Complex. The extensive Breede River estuary and Blombos Cave lie respectively 10 km and 45 km east/south-east (Fig. 1b).

In KDC archaeological deposits are concentrated behind the dripline and extend over 280 m^2 at a c. 25° slope. A c. 15 m talus slopes seawards at 31.5°. In KDS visible surface deposits extend c. 7 m^2 at a slope of c. 29° behind the dripline. The deposits are severely truncated and the talus lies at 38.5°. It is probable that the natural and archaeological deposits in the cave complex, especially those in KDS, were truncated by mid-Holocene +2–3 m sea levels (Bateman et al., 2004; Compton, 2001). A quartzite cobble beach lies directly below the complex with an extended rocky shoreline and few sandy beaches. Initial excavations in KDC in 2010 yielded Terminal Pleistocene deposits (Albany Industry) radiocarbon dated at c. 14–10 ka (report in prep.). In 2013 several tons of rockfall were removed in the area of the dripline in Klipdrift Cave (Fig. 3). A limited test excavation in the Klipdrift Cave Lower (KDCL) site revealed MSA deposits underlying the overburden. A provisional minimum OSL age of c. 70 ka was obtained for the base of the overburden. Further excavations of KDCL are planned.

KDS was first excavated in 2011 with subsequent seasons in 2012 and 2013. In total a volume of 2.3 m^3 over an area of 6.75 m^2 has been excavated at KDS to depths from 30 cm to 100 cm (in individual quadrates) and more than 20 layers and lenses defined (Figs. 3 and 4). The uppermost dated layer yields an optically stimulated luminescence (OSL) age of 51.7 ± 3.3 ka, the middle layers containing the HP range from 65.5 ± 4.8 ka to 59.4 ± 4.6 ka and the lowermost excavated, anthropogenically sterile layers give an age of 71.6 ± 5.1 ka (Fig. 4a).

1.2. Background: De Hoop Nature Reserve

De Hoop Nature Reserve covers 34 000 ha and extends for 60 km along the Indian Ocean coastline (Fig. 1b). The Potberg range, a 611 m high remnant of a syncline of the Cape Folded Belt composed of highly resistant TMG quartzite, lies to the north-west of Klipdrift. A major fault at the base of the range truncates it to the south. The TMG quartzites form sea cliffs where they are exposed beneath the Bredasdorp Group limestone. Sedimentary rocks of the TMG (sandstones), Bokkeveld Group (shales) and Uitenhage Group (mainly shale conglomerates) form the basement geology of the area. Marine transgressions have planed the softer shales and conglomerates into a gently southward sloping series of terraces. The Neogene limestones of the Bredasdorp Group, deposited as shallow marine environments (the Pliocene De Hoopvlei Formation and the Pleistocene Klein Brak Formation, both of which are shelly quartzose sand and conglomerate) and as coastal dunes (the Pliocene Wankoe Formation and the Pleistocene Waenhuiskrans Formation), underlie the greater part of the reserve (Marker and Craven, 2002) and cover most of the Bokkeveld and Uitenhage basement rocks. The Wankoe Formation forms the high-lying aeolianites into which the coastal plain was eroded during marine transgressions. More recent dune systems (Waenhuiskrans formation) were subsequently formed on the coastal plain. The Strandveld Formation, deposited as a strip of unconsolidated dunes during the Holocene is the most recent member of the Bredasdorp Group (Bateman et al., 2004; Malan, 1990; Roberts et al., 2006; Rogers, 1988).

The reserve is situated in the Cape Floristic Region, one of the six floral Kingdoms in the world. It falls within a winter rainfall area that has a Mediterranean climate. The current mean annual rainfall is approximately 380 mm with the maximum in August and the minimum in December and January. The warm Agulhas current results in temperate winters and warm summers with an average of 20.5 °C during the latter and an average of 13.2 °C during winter. The continental shelf, known as the Agulhas Bank (Fig. 1b), begins as a relatively shallow topographical feature south of Port Elizabeth and extends to the south and west beyond Cape Agulhas, 80 km west of the Klipdrift Complex. At its widest point, south of Cape Infanta (Fig. 1b), the Agulhas Bank extends more than 200 km (Bateman et al., 2004; Carr et al., 2007; Compton, 2011; Van Andel, 1989).

Three major vegetation types occur in the reserve, Limestone Fynbos, Mountain Fynbos, and Dune Fynbos/Thicket (Low and Rebelo, 1996). A diversity of plants and animals, both terrestrial and marine in a complex mosaic of different habitat types, is a result of these varied geological features and the close location of the reserve to Cape Agulhas, the meeting point of the west coast cold Benguela and warm east coast subtropical Agulhas currents. This diversity is illustrated by the 86 terrestrial mammal species that occur here, at least 250 species of fish in the marine protected area and the more than 260 resident and migratory bird species. Limestone Fynbos, which is characterized by low shrubs, is the predominant vegetation in the immediate vicinity of the Klipdrift Complex (Willis et al., 1996).

2. Excavation methodology

Two grid systems, oriented on a local north–south axis, were set up using a Trimble VX Spatial Station. The first is a three-

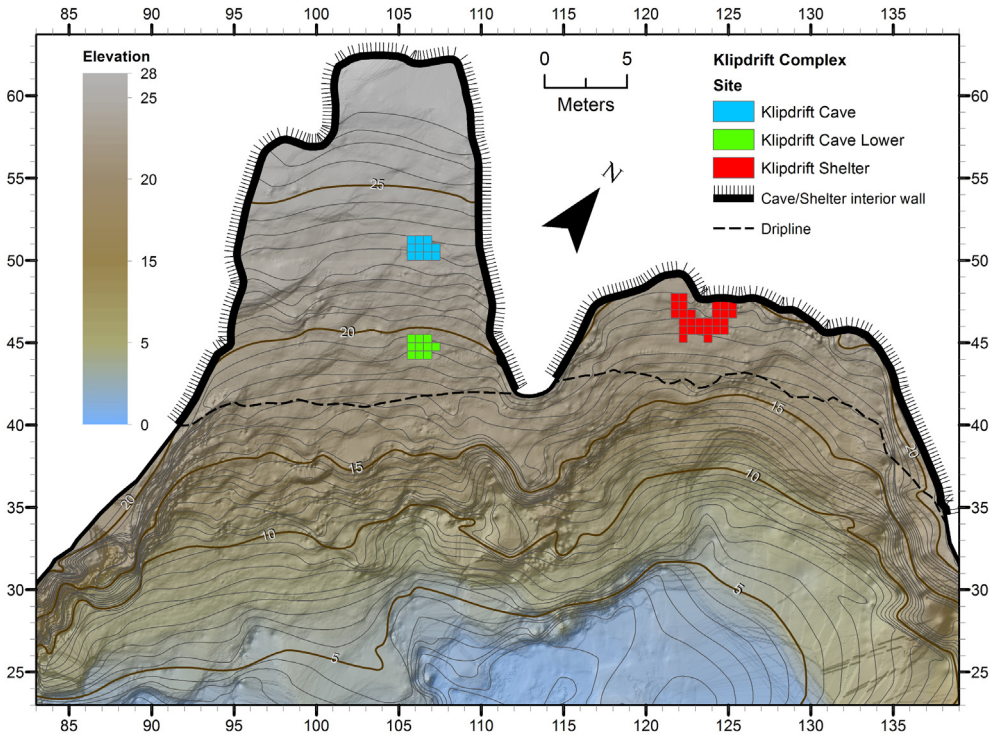

Fig. 3. Topographical features of Klipdrift Complex including layout of excavated archaeological sites, Klipdrift Cave, Klipdrift Cave Lower and Klipdrift Shelter.

dimensional, numerical coordinate system, where the X and *Y* axes are given arbitrary numerical values (50, 100), and the *Z* axis values refer to elevation above sea level. The second, an alpha-numerical system, consists of a continuous square metre grid starting from A1, in which each square is further subdivided into four 50 × 50 cm quadrates (named a, b, c and d) (see Fig. 4b).

Each quadrate was excavated individually by brush and trowel, following stratigraphic layers. The layers within each quadrate which contain sediments of several depositional events were principally identified and defined by their texture, composition, colour, thickness and content. The spatial extent of individual layers varies throughout the excavated area and layer depths range from c. 2–30 cm. The layers were given alphabetically ordered name codes (PAL, PBA, PCA etc.) (see Fig. 4). Name codes that share the two first letters (e.g. PA and subdivisions PAL, PAM etc.) were interpreted as having close contextual relationships. A micromorphological study of these layers is in progress. Spatial measurements taken during excavation refer to the numerical coordinate and were given a three-dimensional (XYZ) spatial reference. Lithics >20 mm, identifiable bones, ostrich eggshell, ochre and artefacts of special interest were individually recorded with high precision (1/1000 cm) and with an accuracy of ±2 mm. Recovered finds or features were bagged in plastic, labelled with provenance data and given a unique specimen number. All plotted finds were classified on a primary entry form in the field by raw material, species, tool type and special characteristics. Non-plotted material (deposit/sediments) was sieved through a nested 3.0–1.5 mm sieve and retained for future analysis.

The topographic surface of a stratigraphic layer in a quadrate was recorded by c. 500 3D points (point cloud) using the 3D scanning function on the Trimble VX spatial station. The point cloud was later converted into a 3D model of the entire layer surface for remodelling of the original surface topography. The surface of each quadrate was also digitally photographed with a single lens reflex camera (Nikon D4) with surface markers, permitting the image to be geo-referenced and modelled in 3D. Similar photos were taken of section walls, significant artefacts *in situ* and other relevant features.

All site maps, cross sections and illustrations of the KDS stratigraphic sequence are geo-referenced within the numerical coordinate system and made by combining photogrammetric methods with topographic data recorded by the total station. The Klipdrift Complex and surrounds were mapped by scanning the site in 3D. The point cloud that was generated (c. 250 000 points) was imported into Trimble RealWorks 6.5 and converted into a 3D mesh, from which planar maps, cross-section of surface topography and elevation models were produced. These were subsequently exported as CAD files and imported into ESRI ARCGIS 10.1 for further refinement, map making and for combining with geo-referenced images (Figs. 3 and 4). Materials recovered from the sites were primarily sorted and washed at the base laboratory situated at Potberg in the De Hoop Nature Reserve. On completion of the excavations, the material was moved to our laboratory in Cape Town for curation and further investigation. In the longer term the recovered assemblages will be curated at the Iziko South African Museum in Cape Town.

3. Optically stimulated luminescence dating

The MSA layers at KDS were dated using single-grain OSL. Single-grain measurements were performed since previous OSL dating studies conducted on southern African MSA sites demonstrate that multi-grain analyses are susceptible to a number of sources of inaccuracy (e.g. Jacobs et al., 2008). These inaccuracies may be avoided by measuring and analysing the OSL properties of a sample at the single-grain level (Jacobs and Roberts, 2007).

3.1. Sample collection, preparation and measurement

Samples were collected from cleaned sections by scraping material into opaque bags while under tarpaulin. Sample locations are listed in Table 1. Using the procedure outlined in Armitage et al.

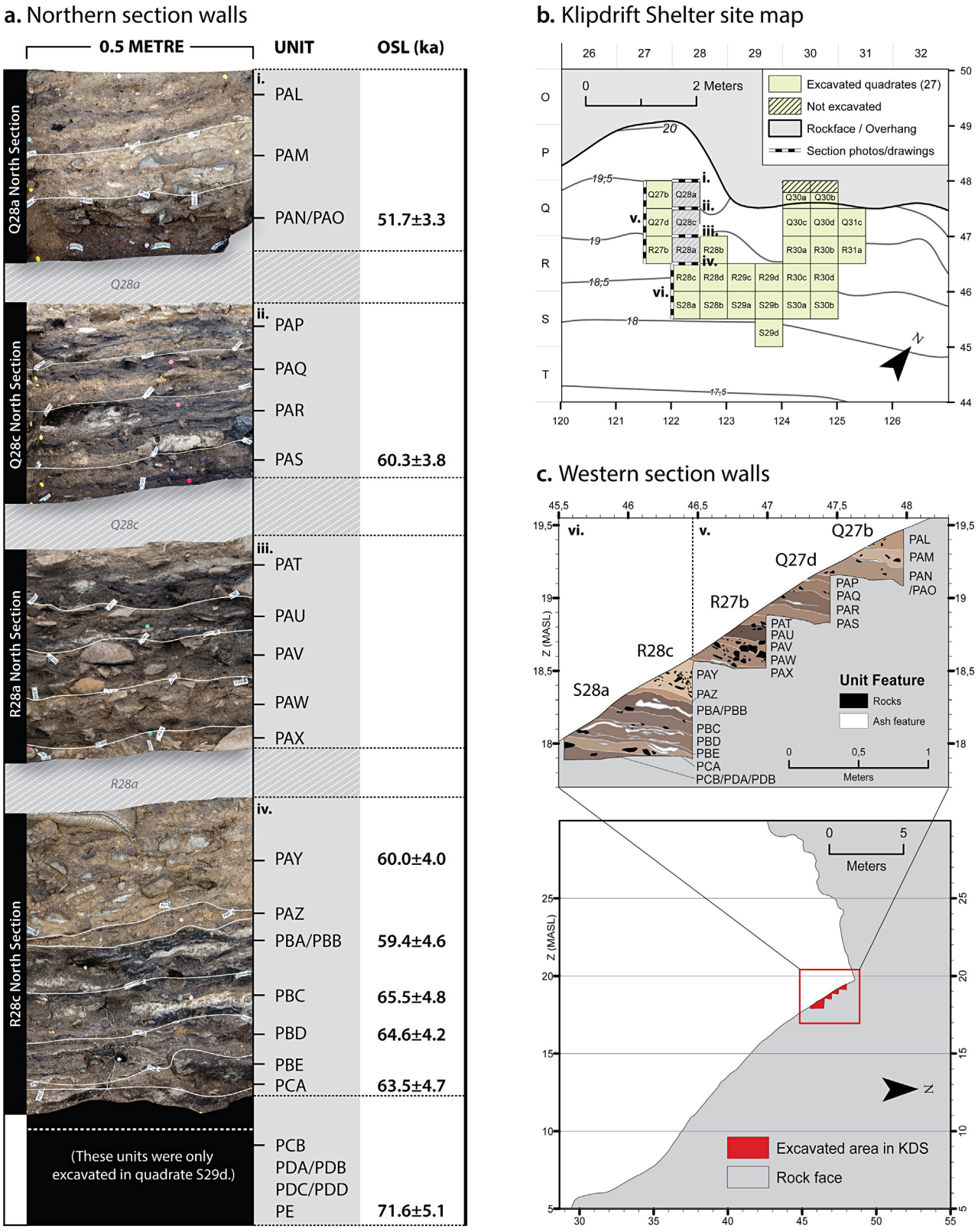

Fig. 4. a) Stratigraphy of Klipdrift Shelter showing layers and optically stimulated luminescence ages; b) Location of excavated quadrates within KDS; c) excavated layers in section showing the slope.

(2011) 212–180 μm diameter quartz grains were extracted from bulk samples. Beta and gamma dose rates were calculated for each sample using radioisotope concentrations measured by ICP-MS (U and Th) and ICP-AES (K). Dose rates were corrected using an assumed water content of 20 ± 5%. This assumed value was preferred to measured values since the latter are strongly dependent upon the time elapsed since the section was excavated and the antecedent weather conditions. The assumed value is close to the mean measured water content (19 ± 6%) for a suite of 12 samples from KDS, which with the inclusion of the 5% uncertainty term, gives confidence that it approximates the true mean burial conditions. Gamma dose rates were corrected for a 20% volume of low-radioactivity clasts. Cosmic ray dose rates were calculated using site location and overburden density, accounting for shielding by the nearby rock face (Prescott and Hutton, 1994; Smith et al., 1997). An internal alpha dose rate of 0.03 ± 0.006 Gy/ka was assumed.

Equivalent doses were measured using the single-aliquot regenerative-dose technique (Murray and Wintle, 2000) using a Risø TL/OSL-DA-15 instrument (Bøtter-Jensen et al., 2003) fitted with a single-grain OSL attachment (Duller et al., 1999, 2000). Single-aliquot dose recovery tests (Roberts et al., 1999) were performed on every sample, and indicate inter-sample variability in the optimal preheating regime, a phenomenon also observed at Diepkloof Rock Shelter (Tribolo et al., 2013). Single-grain dose recovery tests, using the optimal measurement conditions identified by the single-aliquot data, were performed on four samples and yielded dose recovery ratios consistent with unity. Equivalent dose (D_e) measurements were performed using the optimal preheating regime identified for each sample. Data were screened using the grain rejection criteria of Armitage et al. (2011). In addition, grains were rejected where the sensitivity-corrected natural luminescence intensity exceeded twice the D_0 value of the saturating exponential fit to the growth curve (Wintle and Murray, 2006; Chapot et al., 2012). Equivalent doses were calculated for grains which passed these rejection criteria.

3.2. Estimation of the sample burial dose

All samples yielded sufficient data to calculate a meaningful D_e. Where the overdispersion (σd, the relative standard deviation of the true palaeodoses) of single-grain D_e values for a sample was 20% or less, all grains were assumed to belong to a single population (following Olley et al., 2004), and the Central Age Model (CAM, Galbraith et al., 1999) was used to calculate an equivalent dose for that sample. Where overdispersion exceeded 20%, it was assumed that more than one dose population was present, and the dataset was analysed using the Finite Mixture Model (FMM, Roberts et al., 2000). All datasets to which the FMM was applied were best fitted with two D_e populations, and in each case a single dominant population (≥87% of accepted grains) was identified. The D_e calculated for this population was considered most appropriate for age determination. In samples KDS-DS7, 10 and 11, the remaining grains belong to a small (2–8%) lower dose population, which was interpreted to indicate the intrusion of lower dose grains from above by bioturbation, though it is noteworthy that samples overlying KDS-DS10 (KDS-DS1, 2 and 9) do not contain similar populations. The small (7–13%) higher dose population present in samples KDS-DS1, 2 and 9 was interpreted as indicating the presence of "partially bleached" grains.

Although 20% overdispersion has been widely used as a threshold above which the FMM should be used, it has been argued that this threshold is strictly only applicable to the Olley et al. (2004) dataset. In addition, samples which cannot contain more than one equivalent dose population occasionally yield overdispersion values above 20% (e.g. Armitage and King, 2013). However, inspection of radial plots for samples KDS-DS9 and 10 (Fig. 5a, b) indicates that both the minor high and low De populations identified by the FMM are clearly distinct from the population containing the majority of the grains. Conversely, radial plots for samples KDS-DS 3 and 12 (Fig. 5c, d), which were analysed using the CAM, appear to show a single population of grains. These results indicate that, for our dataset, the correct statistical model may accurately be chosen using the overdispersion parameter. Ages for the KDS samples are presented in Table 1.

4. Cultural artefacts

4.1. Lithics

This preliminary techno-cultural interpretation of the KDS sequence is based on the lithics recovered in 2010 and 2011. Layers PCA to PAY, ranging from 65.5 ± 4.8 ka to 59.4 ± 4.6 ka, provide highly significant samples for a first technological assessment, with 11,687 lithics >2 cm in the seven layers considered here (Table 2).

Lithic raw materials are composed of five main groups: quartzite, quartz, silcrete, cryptocrystalline silicate (CCS) and calcrete. In all layers, a large portion of the stone found derives from the shelter's walls, and are mostly quartzite and to a lesser extent quartz. These coarse and poor quality raw materials were occasionally exploited by the knappers. Quartzite also includes fine-grained types derived from pebbles, while quartz is predominantly composed of good quality types, with very fine crystalline structure. Silcretes used by the KDS tool-makers are almost exclusively fine-grained types, frequently with internal cracks. Colour variations include grey, yellow-brown, brown, red and green. Primary sources of silcrete and calcrete are present in abundance along the Cape Fold Mountains (see Roberts, 2003) and near KDS they occur as outcrops in small rocky hills some 10 km north and

Table 1
Summary equivalent dose data and ages for the KDS samples. Samples are listed in stratigraphic order: σd denotes overdispersion, while *n* is the number of grains which pass the rejection criteria. The age models used are the Central Age Model (CAM) and the Finite Mixture Model (FMM). Uncertainties are based on the propagation, in quadrature, of errors associated with individual errors for all measured quantities. In addition to uncertainties calculated from counting statistics, errors due to 1) beta source calibration (3%, Armitage and Bailey, 2005), 2) ICP-MS/AES calibration (3%), 3) dose rate conversion factors (3%), 4) attenuation factors (2%, Murray and Olley, 2002) have been included.

Sample (KDS-…)	Square	Level	σd (%)	*n*	Age model	Grains in main component (%)	Equivalent dose (Gy)	Dose rate (Gy/ka)	Age (ka)
DS11	Q27B	PAN/PAO	25 ± 3	146	FMM	98 ± 1	45.4 ± 1.2	0.88 ± 0.04	51.7 ± 3.3
DS12	Q27B	PAS	18 ± 3	126	CAM	100	52.1 ± 1.4	0.86 ± 0.04	60.3 ± 3.8
DS3	R28C	PAY	19 ± 3	81	CAM	100	59.1 ± 1.9	0.98 ± 0.05	60.0 ± 4.0
DS2	R28C	PBA/PBB	27 ± 4	65	FMM	93 ± 6	54.8 ± 2.4	0.92 ± 0.05	59.4 ± 4.6
DS1	R28C	PBC	27 ± 3	113	FMM	87 ± 9	45.2 ± 1.9	0.69 ± 0.04	65.5 ± 4.8
DS9	R28C	PBD	21 ± 3	111	FMM	87 ± 5	58.5 ± 1.5	0.91 ± 0.05	64.6 ± 4.2
DS10	R28C	PCA	21 ± 3	60	FMM	95 ± 4	71.6 ± 3.0	1.13 ± 0.06	63.5 ± 4.7
DS7	S30A	PE	31 ± 4	91	FMM	92 ± 4	74.8 ± 2.9	1.05 ± 0.05	71.6 ± 5.1

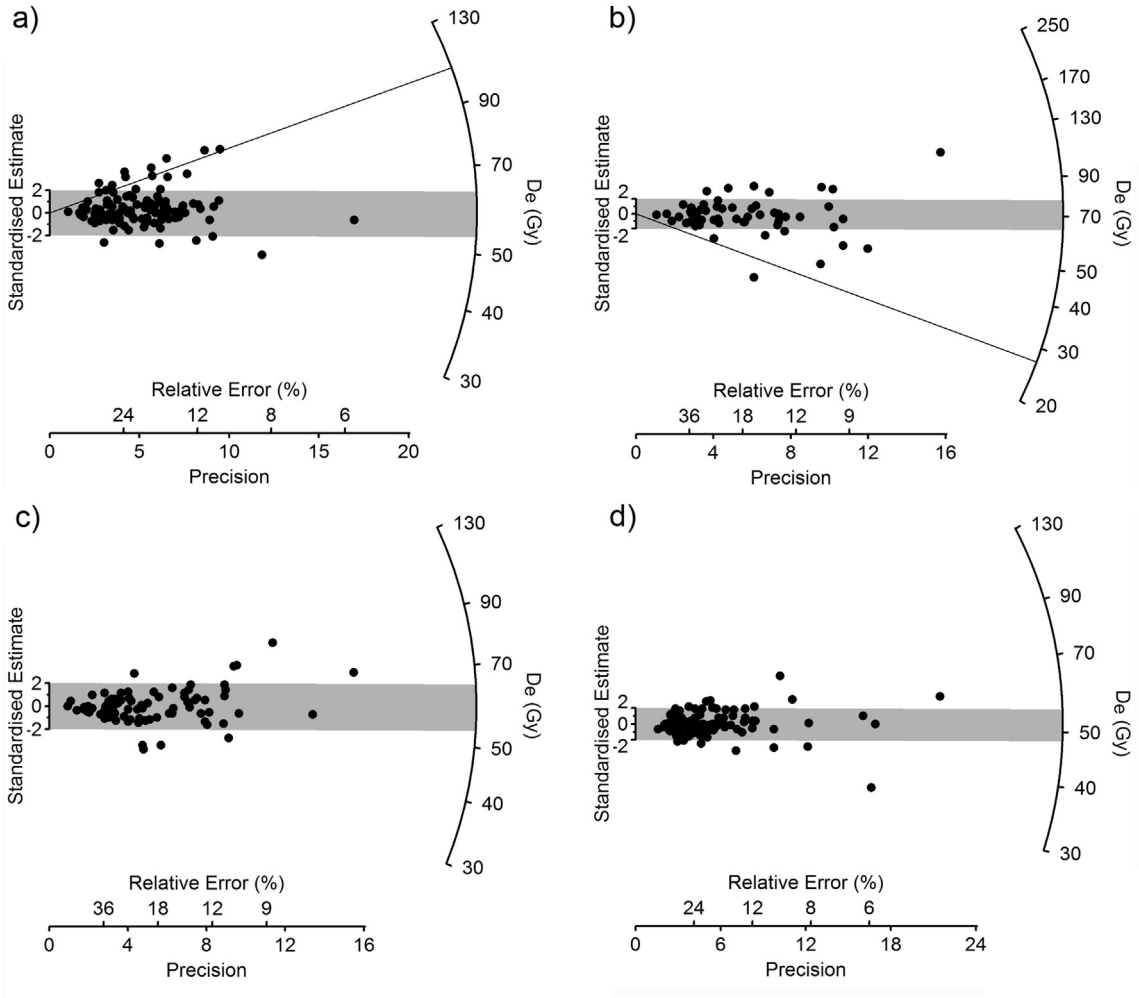

Fig. 5. Radial plots of equivalent doses for a) KDS-DS9, b) KDS-DS10, c) KDS-DS3 and d) KDS-DS12 of remaining deposits.

north-west of the site. Some of the knapped silcrete may originate from pebble sources that have not yet been identified.

Significant changes occur in the relative proportions of these raw material groups over time. Silcrete is dominant in the three lower layers (PCA, PBE, PBD), while quartz increases significantly in the two overlying layers (PBC, PBA/PBB), and quartzite as well as calcrete become more abundant in the uppermost PAZ and PAY layers (Table 2 and Fig. 6). These shifts in the sequence are even more pronounced when considering the raw material distribution of the blades and formal tools (backed tools and notched tools in particular) (Fig. 6).

The lithic *chaîne opératoire* performed on quartz, silcrete and CCS is almost entirely devoted to the production of blades, which is confirmed by the strong predominance of blade cores in all layers (PCA: 16/21 cores, PBE: 9/12, PBD: 35/47, PBC: 21/29, PBA/PBB: 26/43, PAZ: 11/18, PAY: 9/17). The flaking method applied to blade production is almost exclusively unidirectional and a number of technical attributes, e.g. platform edge abrasion, weakly developed bulbs and thin platforms, indicate the use of direct marginal percussion with a soft hammer, either mineral or vegetal. Core volume exploitation is varied and includes unifacial cores with prepared lateral convexities, semi-rotating cores, "narrow-face" cores and bipolar cores. The mean width of blades is quite homogeneous across raw materials and tends to be slightly higher in the four uppermost layers (from PBC to PAY: Fig. 6). The elongation of blades is high in all layers, with no significant pattern of change over time (blades' length/width in PCA: 2.7, PBE: 2.4, PBD: 2.5, PBC: 2.7, PBA/PBB: 2.3, PAZ: 2.4, PAY: 2.5). Blades (Fig. 7: 1–12) range from very small (length between 10 and 20 mm) to large (over 60 mm in length). Besides blade production, secondary flake production occurs on quartz, silcrete and calcrete. It consists mainly of discoidal and Levallois débitage. Discoidal cores occur in small quantities in the whole sequence, unlike the Levallois cores which are limited to the upper part of the sequence (layers PBC, PBA/PBB, PAZ, and PAY). The existence of a secondary Levallois reduction sequence is confirmed by the presence of Levallois flakes. These are very rare or absent from layers PCA to PBA/PBB and amount to 5 Levallois flakes in PAZ, and 24 in PAY. The top part of the sequence thus provides evidence for the emergence of an independent and structured flake reduction sequence. In contrast to other raw materials, quartzite was predominantly used for producing flakes (Table 2) from informal and unidirectional cores. Blade production on quartzite is weakly developed in all layers, except in PAY where quartzite blade production is relatively well represented. For both flake and blade production, quartzite exploitation was based on expedient and short reduction sequences performed with direct hard hammer percussion.

The tools (Fig. 7: 13–27) are typical of the HP; formal tools are composed of backed tools, notched tools, borers, retouched blades, *pièces esquillées* and points. Retouched tools account for less than 5% of the assemblages (PCA: 3.5%, PBE: 2.5%, PBD: 2.8%, PBC: 3.2%, PBA/PBB: 3.2%, PAZ: 5%, PAY: 2.6%). Some marked shifts occur in the

Table 2
Assemblage composition at KDS (the chunk category, which accounts for c. 40% of the total assemblage, has been eliminated from the quantitative analyses as it includes a number of ambiguous items – natural slabs or knapping debris – especially for quartzite).

	PAY		PAZ		PBA/PBB		PBC		PBD		PBE		PCA	
	n	%	*n*	%	*n*	%	*n*	%	*n*	%	*n*	%	*n*	%
Flakes														
Quartz	67	8.9	178	33.9	631	40.9	152	23.6	145	7.9	81	10.2	104	13.9
Silcrete & CCS	97	12.9	60	11.4	71	4.6	44	6.8	250	13.6	79	10	97	12.9
Calcrete	34	4.5	15	2.9	59	3.8	1	0.2	0	0	6	0.8	0	0
Quartzite	318	42.3	136	25.9	316	20.5	265	41.1	560	30.4	204	25.8	220	29.3
Blades														
Quartz	22	2.9	35	6.7	312	20.2	66	10.2	150	8.1	117	14.8	66	8.8
Silcrete & CCS	69	9.2	32	6.1	29	1.9	44	6.8	556	30.2	238	30.1	186	24.8
Calcrete	15	2	9	1.7	17	1.1	0	0	3	0.2	0	0	1	0.1
Quartzite	88	11.7	16	3	29	1.9	27	4.2	80	4.3	36	4.5	36	4.8
Cores														
Quartz	10	1.3	8	1.5	41	2.7	17	2.6	14	0.8	6	0.8	9	1.2
Silcrete & CCS	7	0.9	10	1.9	4	0.3	9	1.4	34	1.8	6	0.8	7	0.9
Calcrete	5	0.7	0	0	1	0.1	0	0	0	0	0	0	0	0
Quartzite	4	0.5	1	0.2	0	0	4	0.6	8	0.4	0	0	0	0
Tools														
Quartz	0	0	6	1.1	23	1.5	10	1.6	7	0.4	0	0	2	0.3
Silcrete & CCS	9	1.2	12	2.3	6	0.4	4	0.6	32	1.7	15	1.9	20	2.7
Calcrete	2	0.3	3	0.6	0	0	0	0	0	0	0	0	0	0
Quartzite	3	0.4	2	0.4	4	0.3	0	0	4	0.2	1	0.1	0	0
Hammerstones	1	0.1	2	0.4	1	0.1	2	0.3	0	0	3	0.4	2	0.3
Subtotal	751	100	525	100	1544	100	645	100	1843	100	792	100	750	100
Chunks														
Quartz	141	–	135	–	308	–	83	–	114	–	127	–	89	–
Silcrete & CCS	10	–	22	–	19	–	12	–	48	–	22	–	35	–
Calcrete	25	–	8	–	19	–	5	–	0	–	0	–	0	–
Quartzite	936	–	288	–	548	–	382	–	492	–	522	–	358	–
Pebbles	14	–	12	–	11	–	11	–	8	–	17	–	16	–
Subtotal	1126		465		905		493		662		688		498	
Total	1877		990		2449		1138		2505		1480		1248	

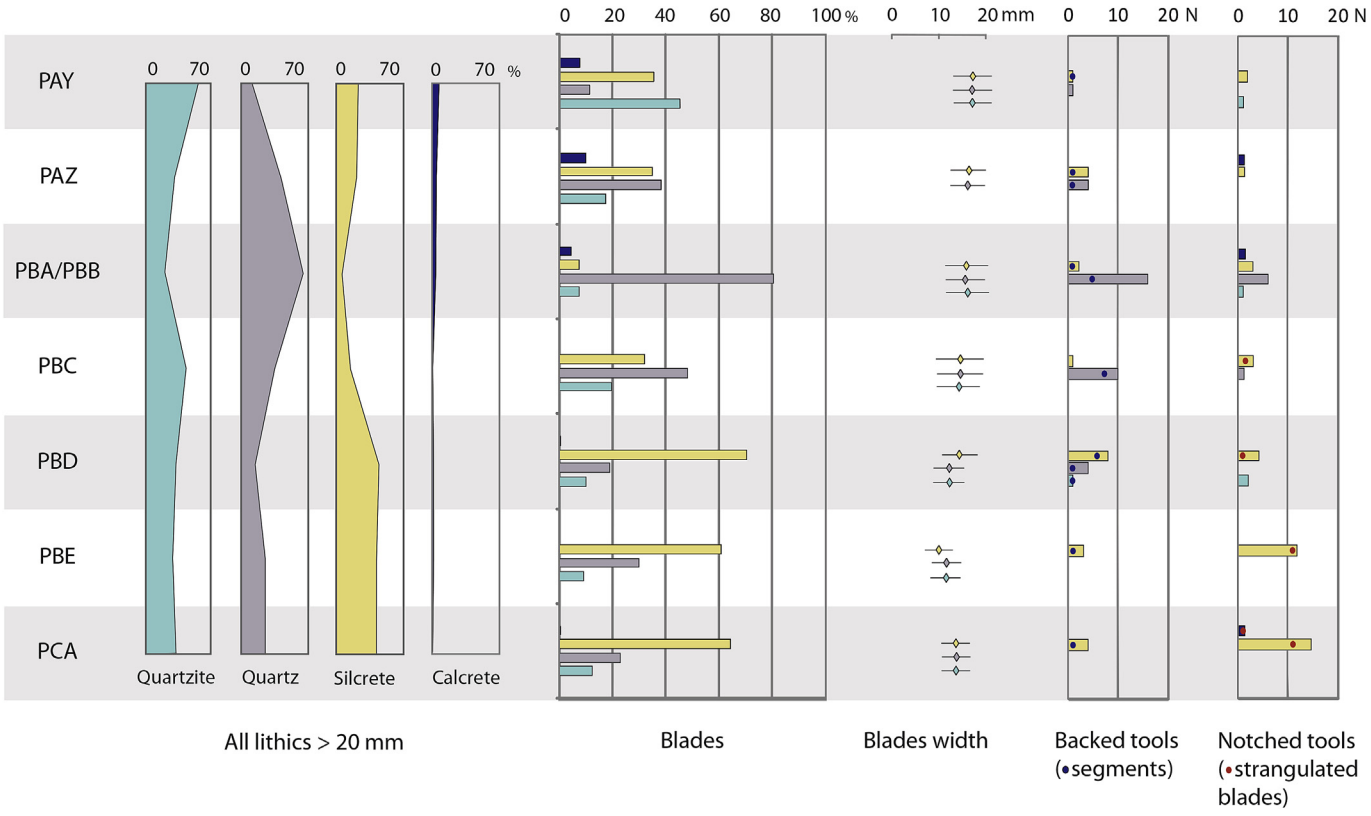

Fig. 6. Technological changes in lithics at KDS, layers PCA to PAY.

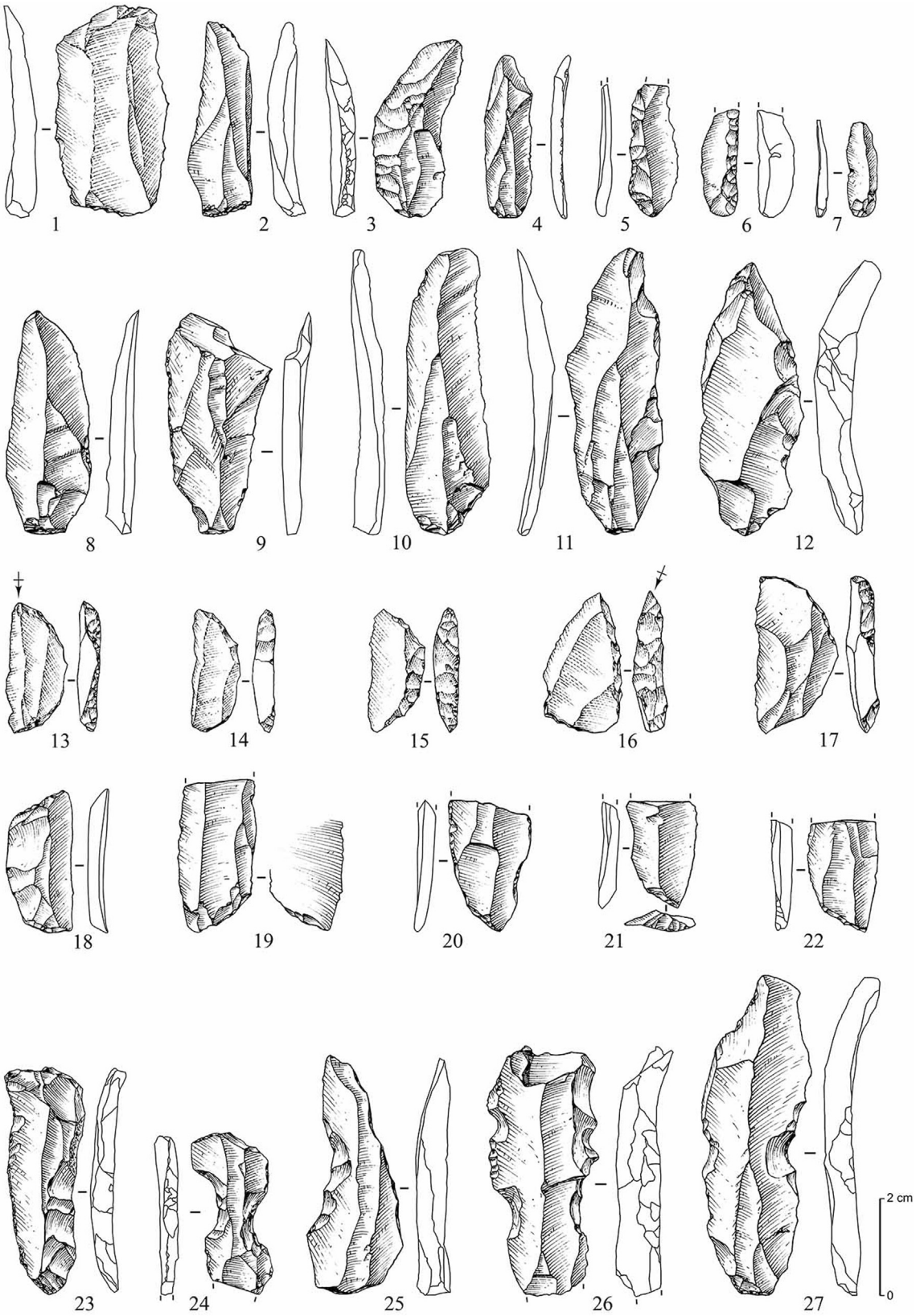

Fig. 7. Blades and formal tools: 1: quartz blade, layer PBA/PBB; 2, 3, 4, 5, 7, 8: silcrete blades, layer PBD; 6, 9: silcrete blades, layer PBC; 10, 11, 12: silcrete blades, layer PCA; 13, 14: quartz segments, layer PBC; 15: quartz segment, layer PBA/PBB; 16: quartz backed tool, layer PBA/PBB; 17: silcrete segment, layer PBD; 18: silcrete bi-truncated tool, layer PBD; 19, 20: silcrete truncated tools, layer PBE; 21,22: silcrete truncated tools, layer PCA; 23, 26: silcrete strangulated notches, layer PBE; 24: silcrete retouched blade, layer PBD; 25: silcrete strangulated blade, layer PBD; 27: silcrete strangulated blade, layer PCA.

toolkit composition over time, both between and within tool groups (Table 3). Backed tools include different types (Fig. 7: 13–22), whose proportions vary consistently from one layer to another. Segments (Fig. 7: 13–15, 17) are best represented in the middle part of the sequence (layers PBD, PBC, PBA/PBB), with a peak in PBC (Fig. 6) where they correspond to a small set of quartz segments ($n = 7$) with standardized morpho-dimensional attributes. Truncated blades (*sensu* Igreja and Porraz, 2013) are present in almost all layers (PCA to PAZ). Within this category, a few highly standardized silcrete tools are characterized by a proximal oblique truncation opposite to a broken transverse distal part (Fig. 7: 19–22), which are only present in the lower layers (PCA – $n = 3$, PBE – $n = 2$, PBD – $n = 1$). Notched tools (Fig. 7: 23, 25–27) are also diagnostic with regard to patterns of change within the sequence (Fig. 6). They represent a large majority of the retouched tools in the lower layers (PCA and PBE with respectively 16/22 and 12/16 notched tools/total of tools). In these two layers, notched pieces include typical strangulated blades (Fig. 7: 23, 25–27) with multiple deep retouched notches on one or two lateral edges of large silcrete blades (PCA – $n = 7$ including 1 calcrete tool, PBE – $n = 6$). They also occur in lesser proportions in PBD ($n = 1$) and PBC ($n = 2$), but are totally absent in the uppermost layers. In all layers, notched tools are predominantly made on silcrete blanks.

The shift from a notched tool-dominated toolkit (in PCA, PBE) to a backed tool-dominated toolkit (in PBC, PBA/PBB) is closely correlated with the inversion of the relative proportions of silcrete to quartz in the same layers (Fig. 6). Few other categories of formal tools are specific to certain layers. PBD in particular contains borers in silcrete ($n = 2$), quartz ($n = 2$, including 1 crystal quartz) and CCS ($n = 1$). Silcrete blades with marginal continuous retouch on one lateral edge (Fig. 7: 24) are almost exclusively present in PBD ($n = 8$), and occur rarely in both PCA ($n = 1$) and PBC ($n = 1$). Unifacial points only occur in PAY ($n = 3$) and are typical of the "post-HP" period in southern Africa (see for instance Conard et al., 2012; Lombard et al., 2012; Soriano et al., 2007; Villa et al., 2005).

Technological variations through time from PCA to PAY relate to three main phases that can be included within the HP complex. The lowermost phase (PCA, PBE) is characterized by the predominant exploitation of silcrete for blade production, the prevalence of notched tools, the presence of strangulated blades and of highly standardized truncated blades. The following phase (PBC, PBA/PBB) is marked by an increase in quartz exploitation which becomes the most common raw material, while backed tools, including typical segments, constitute the main tool group. The third and uppermost phase (PAY) is defined by the predominance of quartzite, an increase in the size of blades, the emergence of an independent and structured flake production based on a Levallois concept, a decrease in the proportions of backed tools and the presence of a few unifacial points. PAY could be interpreted as a transitional layer towards the post-HP. In between these phases, layers PBD and PAZ appear as transitional layers, thus pointing to a process of gradual change over time.

4.2. Ochre

Mineral pigments recovered from archaeological contexts are generally termed 'ochre' and refer to rocks which derive their colour from haematite (α – Fe) and goethite (α – FeO(OH)) (Eastaugh et al., 2008). The term describes earthy materials which consist of anhydrous iron (III – ferric or Fe^{3+}) oxide such as red ochre (unhydrated haematite or Fe_2O_3), partly hydrated iron (III) oxide-hydroxide such as brown goethite (FeO(OH)) or hydrated iron (III) oxide-hydroxide such as yellow limonite ($Fe_2O_3(OH)$ nH_2O) (Cornell and Schwertmann, 2003).

An identified total of 356 pieces or 1756 g of ochreous material was extracted during the 2011–2013 excavation seasons at KDS. Ochreous deposits do not occur within the shelter and no sources have been identified in the immediate vicinity of the complex. Besides a ferricrete source 400 m to the east several ochreous outcrops occur within 5–10 km of the site. Ochre sources are more frequent within a 30 km radius of KDS, the most conspicuous being the Bokkeveld Group deposits of the Cape Supergroup (Vorster, 2003). These comprise red ferruginous shales, siltstones, mudstones and haematised shales. The lowering of sea levels, for example during MIS 5e, would likely have exposed Bokkeveld shales within 0.5–1 km from the site.

All identified specimens heavier than 0.1 g were analysed and are described in terms of weight and size, colour, geology and processing technique employed. The analysed pieces comprise both complete (such as hard ferruginous) and fragmentary (softer shales and mudstones) specimens.

4.2.1. Stratigraphic frequency

The bulk of the assemblage derives from layers PBA/PBB followed by PCA and PBD (Table 4). By mass, layer PBE has the highest concentration of red ochre (847.6 g) in the assemblage (48.3%). It should be noted that by weight just over 90% of the ochre in layer PBE consists of coarse to finely processed pieces weighing less than 0.1 g each. In terms of average mass the highest mean weights are recorded in PBC (4.3 g) and PCA (3.2 g). The high standard

Table 3
Retouched tool composition at KDS (Q: quartz, S: silcrete, C: calcrete, Qi: quartzite) (backed tools may include localized or marginal retouch and oblique truncations may also be proximal).

	PAY				PAZ				PBA/PBB				PBC				PBD				PBE				PCA			
	Q	S	C	Qi	Q	S	C	Qi	Q	S	C	Qi	Q	S	C	Qi	Q	S	C	Qi	Q	S	C	Qi	Q	S	C	Qi
Segments	1	–	–	–	1	1	–	–	4	1	–	–	7	–	–	–	1	3	–	1	–	1	–	–	–	1	–	–
Backed tools	–	1	–	–	2	4	–	–	17	1	–	–	1	1	–	–	3	4	–	–	–	3	–	–	–	–	–	–
Oblique truncations	–	–	–	–	1	–	–	–	1	–	–	–	2	1	–	–	–	1	–	–	–	2	–	–	–	3	–	–
Single notches	–	2	–	–	–	1	1	–	3	2	–	–	1	1	–	–	–	1	–	–	–	6	–	–	–	8	–	–
Denticulates	–	–	–	1	–	–	–	–	3	1	2	1	–	–	–	–	–	2	–	2	–	–	–	–	–	1	–	–
Strangulated blades	–	–	–	–	–	–	–	–	–	–	–	–	–	2	–	–	–	1	–	–	–	6	–	–	–	6	1	–
Borers	–	–	–	–	–	–	–	–	–	–	–	–	–	–	–	–	2	3	–	–	–	–	–	–	–	–	–	–
Retouched blades	–	–	–	–	–	–	–	–	–	–	–	–	–	1	–	–	–	8	–	–	–	–	–	–	–	1	–	–
Unifacial points	–	2	–	1	–	–	–	–	–	–	–	–	–	–	–	–	–	–	–	–	–	–	–	–	–	–	–	–
Burins	–	1	–	–	–	2	–	–	–	–	–	–	1	–	–	–	–	–	–	–	–	–	–	–	–	–	–	–
Pièces esquillées	–	–	–	–	–	–	1	–	–	1	–	1	1	–	–	–	1	5	–	–	–	–	–	–	–	–	–	–
Scrapers	–	–	–	1	–	1	1	1	2	2	1	1	1	–	–	–	–	1	–	1	–	–	–	–	–	1	–	–
Miscellaneous	–	5	4	1	4	5	–	1	1	3	–	2	1	–	–	–	–	12	–	–	–	1	–	1	2	3	–	–
Total	1	11	4	4	8	14	3	2	31	11	3	5	15	6	0	0	7	41	0	4	0	19	0	1	2	24	1	0

Table 4
Ochre frequency by weight, size and stratigraphic layer.

Layer	Total (n)	Total (g)	Mean (g)	Std. dev.	Mean (mm)	Std. dev.
PAY	17	13.4	0.8	1.6	16.4	5.7
PAZ	12	21.2	1.8	3.2	16.8	10.4
PBA/PBB	113	248.7	2.2	5.4	15.4	8.3
PBC	19	126.7	4.3	11.5	23.5	14.4
PBD	59	182.2	1.7	5.1	17.4	9.1
PBE	39	847.6	1.6	7.5	12.9	8.8
PCA	97	316.3	3.2	8.9	19.1	10.5
	356	1756.1	2.2	–	17.3	–

deviations in weight for layer PBC and also PCA indicate that specimens range substantially in terms of weight and therefore size, and possibly also in terms of intensity of processing. The lowest average weights occur in layers PAY (0.78 g) and PBE (1.6 g). The heaviest individual pieces derive from layer PCA (79.5 g), followed by PBE (38.5 g), PBC (35.7 g), PBA/PBB (29.2 g) and PBD (17.3 g). The least heavy examples originate from layers PBD, with 41 pieces weighing <0.5 g, and PCA with 36 pieces <0.5 g.

In terms of average size, the largest grouping is that from layers PBC (23.5 mm) and PCA (19.1 mm), followed by PBD, PAZ and PAY at 17.4 mm, 16.8 mm and 16.4 mm respectively (Table 4). Layers PBA/PBB (12.3 mm) and PBE (12.9 mm) contain the smallest mean sizes of ochre pieces. The largest pieces are from layer PCA (74.6 mm) and the smallest from PBA/PBB (1.0 mm). Note the high standard deviations in size for layers PAZ, PBC and PCA.

4.2.2. Geological profiles and colour categories

Six raw material categories are discerned, namely fissile shale, indurated shale, mudstone, ferricrete, haematite and sandstone. Fine-grained and soft (2–3 on Moh's hardness scale) sedimentary forms including fissile shale (53%), indurated shale (22.9%) and mudstone (14.5%) accounts for 90.3% of the raw material assemblage (Fig. 8a). Harder (>4 on Moh's scale) and essentially coarse-grained forms such as ferricrete (2.4%), haematite (2.4%) and sandstone (4.8%) constitute the remainder (9.7%) of the assemblage. Layers PAY to PCA display marked geological variability, with all six geological categories occurring in layers PBC, PBD and PCA. Layer PBC exhibits the highest frequencies of ferricrete (5.3%) and

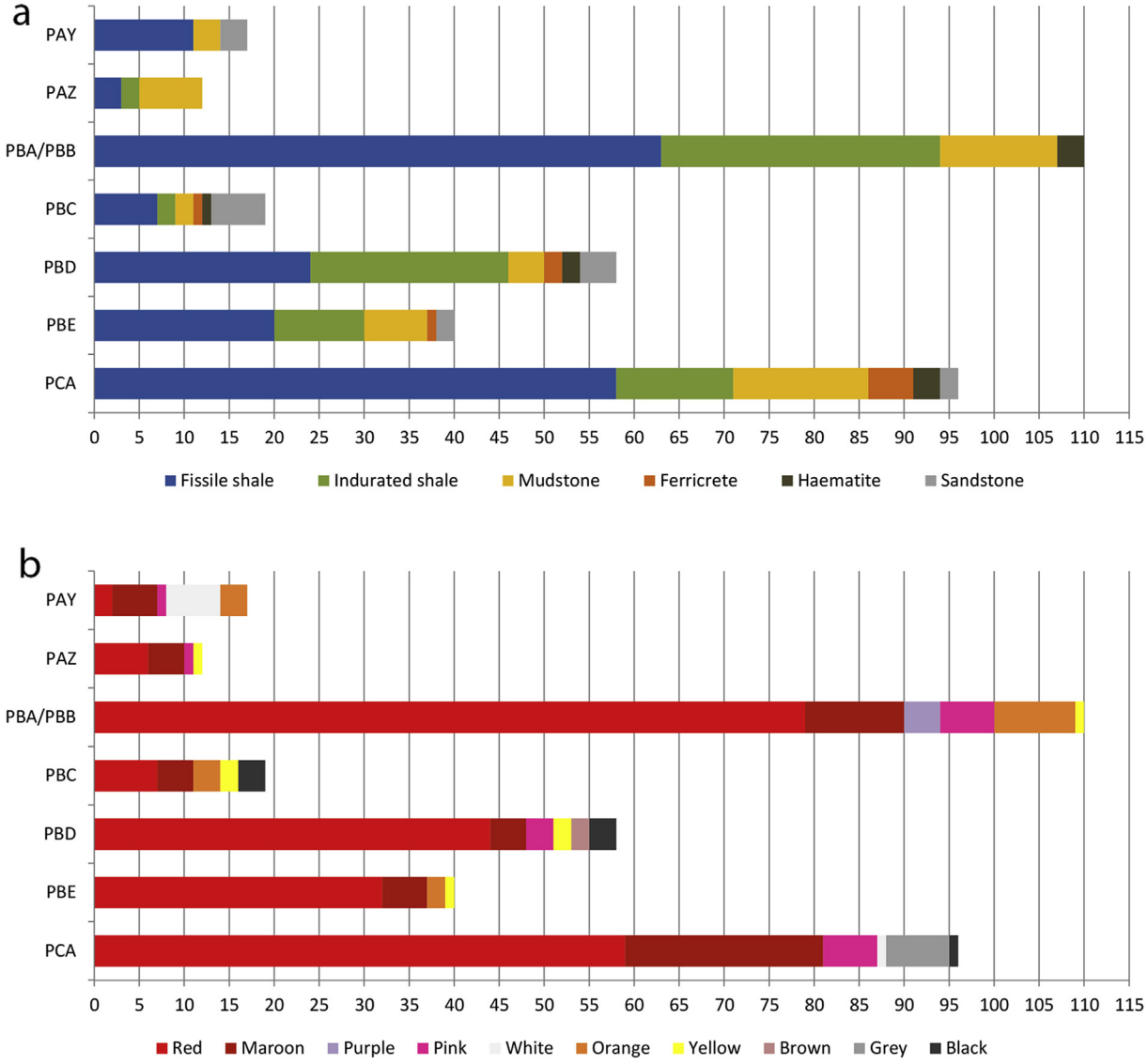

Fig. 8. Ochre recovered from KDS indicated stratigraphically and according to a) raw material frequencies and b) colour. (For interpretation of the references to colour in this figure legend, the reader is referred to the web version of this article.)

Fig. 9. Examples of processed ochre pieces from KDS: a) coarse-grained ground purple shale cobble (PCA), b) ground and polished shale-derived crayon-like piece (PBC), c) ground and scraped soft shale-derived specimen (PCA), d) ground hard shale chunk (PBE) e) knapped and ground haematite-rich shale fragment (PBC). (For interpretation of the references to colour in this figure legend, the reader is referred to the web version of this article.)

sandstone (31.6%). PBE displays the greatest proportion (91.3%) of red ochre derived from fissile and indurated shales.

Colour was collapsed into ten groups including red, maroon, purple, pink, white, orange, yellow, brown, grey and black (Fig. 8b). Geological and colorimetric relationships could not be objectively ascertained, principally because destructive analytical methods are required to determine such variables (Dayet et al., 2013). Basic visual classification and comparison with the Natural Colour System (NCS) Digital Atlas (http://www.ncscolour.com, 2013) was therefore used for colour classification in this study. Although visible spectroscopy can provide the absorbance spectra and colour parameters of the ochre assemblage, this method will only provide information concerning the colorimetric properties of the external surfaces of the specimens. Red (62%) is the predominant colour, followed by maroon (15.3%), orange (4.5%) and pink (4.5%). The remainder of the assemblage (13.7%) includes lighter (yellow and white) and darker (brown and black) categories. The majority (77%) of red pieces are derived from fissile shales.

4.2.3. Utilization strategies

Ochre at KDS occurs in the form of residual powder, nodules, and fragments or as inclusions in larger pieces of rock (Fig. 9). Some examples show signs of grinding on hard abrasive surfaces or scraping with sharp-edged implements. Indications of ochre processing by grinding or scraping ($n = 20$) or by deliberate knapping ($n = 31$) have been identified at KDS.

The proportion of modified pieces (17.5%) is well within the range of other MSA sites (~14%) (Watts, 2002, 2009, 2010; Hodgskiss, 2010; Dayet et al., 2013) (Table 5). Similar to the MSA at Diepkloof (Dayet et al., 2013) Sibudu (Hodgskiss, 2010), Blombos (Watts, 2009) and Pinnacle Point (Watts, 2010), grinding is the primary processing technique. Of the ground pieces including crayons, 67.7% comprise fissile shale, 12.9% indurated shale, 6.5% mudstone and sandstone respectively and 3.2% haematite and ferricrete respectively. Fissile and indurated shales appear to have been preferentially processed by grinding (80.6%). In addition, 81.8% of ochre crayons comprise soft to hard red fissile shales. At Diepkloof and Sibudu scraping is not a primary processing technique and the presence of only a single scraped piece at KDS (layer PBD) is therefore not unusual. Clear indications of knapping occur on 31 pieces from layers PBA/PBB ($n = 20$), PBD ($n = 5$), PBE ($n = 1$) and PCA ($n = 5$), suggesting that knapping may have formed part of the chaîne opératoire of ochre processing in these layers (Fig. 9e).

Table 5
The prevalence of processed ochre pieces per layer.

Layer	*n*	Ground	%	Crayons	%	Flakes	%
PAY	17	1	5.9	–	–	–	–
PAZ	12	1	8.3	–	–	–	–
PBA/PBB	113	6	3.9	3	3.9	20	19.6
PBC	19	4	21.1	2	10.5	–	–
PBD	59	1	3.4	2	3.4	5	8.5
PBE	39	1	2.6	1	2.6	1	2.6
PCA	97	5	6.2	3	2.1	5	5.2
	356	19	6.2	11	3.0	31	8.3

4.3. Ostrich eggshell

We have identified 95 fragments of clearly and deliberately engraved ostrich eggshell (EOES) recovered from layers PAY to PCA (3.8% of the total number of OES fragments). The majority of the EOES pieces derive from PBC (27%) and PBD (25%) (Table 6). An additional 6 engraved pieces were recovered from layer PAX (not reported here), and no EOES fragments were recovered from any of the layers above PAX. The EOES is spatially distributed across the area where HP layers were excavated (4.75 m^2) and up to 50 cm below the surface. There are no LSA deposits in KDS and during excavation there was no sign of disturbance to the deposits that might have resulted from the intrusive burial of engraved eggs at the site by LSA people. The EOES fragments are under study but preliminary observations can be made. The designs entail variations of cross-hatched or sub-parallel line themes, and most are similar to those reported from Diepkloof in the HP and pre-HP layers (Texier et al., 2010, 2013) and from the HP layers at Apollo 11 (Vogelsang et al., 2010). All the designs identified at Diepkloof (Texier et al., 2013, Table 4: 3423) are present at KDS, except for the "sub-parallel intersecting lines motif". One design present in the upper layers at KDS, not reported from Diepkloof, consists of a finely carved diamond shaped cross-hatched pattern (Fig. 10a,b), distinctly different to those from layers below, and from the "crosshatched grid motif" reported from Diepkloof (Texier et al., 2013: 3420). This diamond shaped pattern is present only in layers PAX, PAY and PAZ. In PAX and PAY this is the only engraved

Table 6
Frequency of engraved and unmodified OES throughout the sequence.

Layer	EOES (*n*)	OES (*n*)	% EOES
PAY	5	106	4.7
PAZ	15	187	8.0
PBA/PBB	22	1274	1.7
PBC	23	349	6.6
PBD	25	202	12.4
PBE	4	90	4.4
PCA	1	282	0.4
Total	95	2490	3.8

motif present. The "sub-parallel rectilinear or curved lines" design at Diepkloof (Texier et al., 2013: 3423) is the most commonly occurring motif in layers PBC to PAZ at KDS. Our study of the EOES is ongoing but initial observations suggest similarities with many of the EOES motifs found at Diepkloof, with some differences.

5. Fauna

5.1. Macrofauna

A preliminary analysis of the macrofaunal remains from the PAY to PCA layers was conducted following Driver (2005) and Klein and Cruz-Uribe (1984). The comparative faunal collections of the Ditsong Museum of Natural History in Pretoria were used to identify bone remains. Micromammals, defined as species where adults weigh less than 750 g, are not included in this analysis. Because of the difficulty in differentiating bovids, many remains were assigned only to size classes based on Brain (1974). Size class 1 includes small bovids such as Cape grysbok (*Raphicerus melanotis*), size 2 includes southern reedbuck (*Redunca arundinum*), size 3 includes red hartebeest (*Alcelaphus buselaphus*), and size 4 are large bovids such as eland (*Tragelaphus oryx*) and African buffalo (*Syncerus caffer*). Although eland is sometimes identified as *Taurotragus oryx*, we follow the classification scheme of Skinner and Chimimba (2005) – based on genetic studies (e.g., Essop et al., 1997) – and classify eland as *Tragelaphus oryx*. We also use the size 5 class for very large bovids, such as the extinct long-horned buffalo (*Syncerus antiquus*). Long-horned or giant buffalo are also known as *Pelorovis antiquus* but we follow more recent studies that assign them to the genus *Syncerus* (Gentry, 2010; Rector and Reed, 2010; Faith, 2013). Due to the fragmentary nature of the assemblage, many mammal remains such as rib, cranial or vertebral fragments could not be identified beyond class. These specimens are classified as 'small', 'medium', 'large' or 'very large mammal' based on size. Small mammals are defined as indeterminate specimens ranging in size from the Cape dune molerat (*Bathyergus suillus*) up to and including size 1 bovids, medium mammals up to size 2 bovids, and large mammals are size 3 bovids and larger (Brain, 1974). 'Very large mammal' includes a specimen that could not be confidently identified to order and may be black rhinoceros (*Diceros bicornis*) or long-horned buffalo. Small carnivores range in size to that of the African wild cat (*Felis silvestris*), medium carnivores to the size of the African civet (*Civettictis civetta*) and large carnivores as larger than *C. civetta*. A few fish remains were recovered at KDS, mainly vertebrae and jaw bones, but these have not been studied.

5.1.1. Assemblage

Of the 28,128 fragments of bone, weighing 11,758 g, 2129 (7.6%) could be identified to at least the class level, while 292 (1.0%) could be identified to genus/species. Bone from KDS is extensively fragmented: the majority of identified fragments ($n = 1343$; 63.1%) are less than 2 cm in length and 19.7% of identified bone ($n = 419$) is less than 1 cm long. This extensive fragmentation is likely the reason why the Minimum Numbers of Individuals (MNI) in all layers is lower than expected (Marshall and Pilgram, 1993). Fragmentation is probably a result of burning with evidence present on 1761 fragments (82.7% of identified bone). Although burning was not recorded for unidentified bone, the proportion of unidentified burnt specimens appears much the same as in the identified sample. The elevated proportion of burnt bone is likely due to the high numbers of hearths and hearth-like structures occurring at KDS. Most of the faunal material was recovered from within, or close to, these hearths suggesting that most of the burnt bone can be associated with cooking events. This, and the relative lack of carnivores, is a strong indicator that humans were the main accumulators of the faunal assemblage.

5.1.2. Identified fauna

Tortoise remains are common and constitute 31% of the identified fauna (Table 7). The majority of identified tortoise bones are carapace or plastron but due to their small size it was not possible to differentiate tortoise taxa based on shell fragments. Most of these are likely angulate tortoise (*Chersina angulata*), although some may be the Cape tortoise (*Homopus* sp.). Rock hyrax (*Procavia capensis*) is the most prevalent identified macromammal. Layers

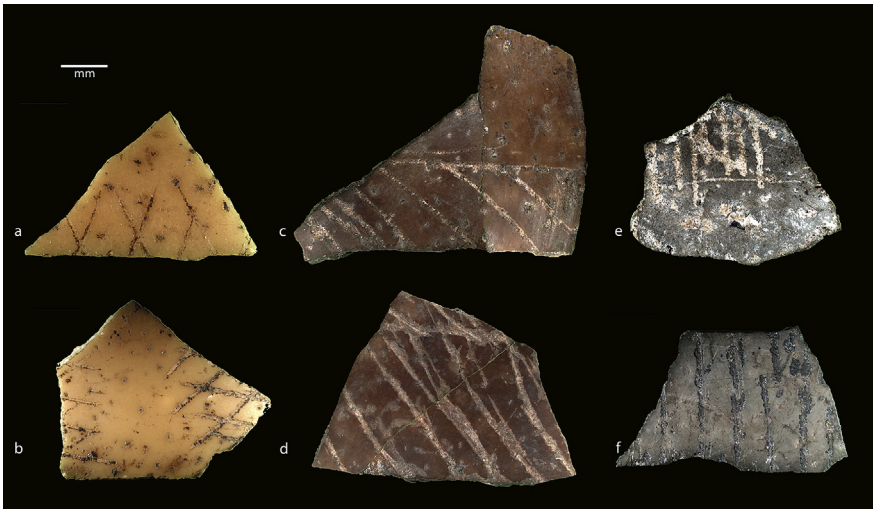

Fig. 10. Engraved OES pieces from PAZ (a and b), PBC (c and d) and PBD (e and f). Note that both c and d consist of two refitted parts.

Table 7
The Number of Identified Specimens (NISP) and the Minimum Number of Individuals (MNI) for macromammal and tortoise remains. Bovid size classes exclude specimens that could be identified to genus/species. Small, medium, large and very large mammals include specimens such as cranial, rib and vertebral fragments that could not be confidently identified beyond class. Linnaean classification based on Skinner and Chimimba (2005) except Syncerus antiquus (Gentry, 2010).

Taxa	Common name	PAY		PAZ		PBA/PBB		PBC		PBD		PBE		PCA	
		MNI	NISP	MNI	NISP	MNI	NISP	MNI	NISP	MNI	NISP	MNI	NISP	MNI	NISP
Testudinidae	Tortoise	2	59	1	23	2	71	2	51	3	251	2	105	1	24
Chersina angulata	Angulate tortoise	2	10	2	4	2	8	2	11	2	21	2	8	1	3
cf. Pelomedusidae	Turtle	–	–	–	–	–	–	–	–	1	1	–	–	–	–
Lagomorpha	Hare/Rabbit	1	1	–	–	–	–	2	4	1	3	–	–	1	3
Lepus saxatilis	Scrub hare	–	–	–	–	–	–	–	–	–	–	–	–	1	1
Lepus sp.	Hare	–	–	–	–	–	–	1	1	1	1	–	–	–	–
Bathyergus suillus	Cape dune molerat	2	8	1	1	–	–	–	–	–	–	–	–	–	–
Procavia capensis	Rock hyrax	3	22	2	11	1	1	3	27	2	30	1	1	1	6
	Small mammal	3	41	2	8	3	33	3	78	3	78	2	8	2	31
Herpestidae sp.	Mongoose	–	–	–	–	–	–	–	–	1	1	–	–	–	–
	Small carnivore	–	–	–	–	1	1	1	2	–	–	1	1	–	–
Felis cf. caracal/serval	Caracal/Serval	–	–	1	1	–	–	1	1	–	–	–	–	–	–
Arctocephalus cf. pusillus	Cape fur seal	–	–	–	–	–	–	–	–	1	2	–	–	–	–
	Medium carnivore	–	–	1	2	–	–	1	1	–	–	–	–	–	–
	Medium mammal	2	16	2	8	3	134	3	80	2	64	2	17	3	30
Parahyaena brunnea	Brown hyena	–	–	–	–	1	1	–	–	–	–	–	–	–	–
Diceros bicornis	Black rhinoceros	–	–	–	–	–	–	1	2	–	–	–	–	–	–
Equus sp.	Zebra	–	–	–	–	2	10	3	25	1	2	–	–	1	2
Raphicerus sp.	Steenbok/Grysbok	1	1	1	1	1	1	2	6	1	7	1	5	–	–
Sylvicapra grimmia	Grey duiker	–	–	–	–	1	2	–	–	1	2	–	–	–	–
Oreotragus oreotragus	Klipspringer	–	–	–	–	–	–	–	–	1	4	–	–	–	–
Ourebia ourebi	Oribi	–	–	–	–	1	1	–	–	–	–	–	–	–	–
Pelea capreolus	Grey (Vaal) rhebok	–	–	1	1	1	3	–	–	–	–	–	–	1	2
Redunca sp.	Reedbuck	–	–	–	–	1	3	–	–	1	1	–	–	–	–
Redunca fulvorufula	Mountain reedbuck	–	–	–	–	1	1	–	–	–	–	–	–	–	–
Redunca arundinum	Southern reedbuck	–	–	–	–	–	–	1	1	–	–	–	–	–	–
Alcelaphini sp.	Hartebeest/Wilderbeest	–	–	–	–	1	3	1	2	1	1	–	–	1	1
Connochaetes gnou	Black wildebeest	–	–	–	–	–	–	1	1	1	1	1	1	–	–
Alcelaphus buselaphus	Red hartebeest	–	–	–	–	1	1	1	1	1	2	–	–	1	1
Damaliscus sp.	Bles or bontebok/?D. niro	–	–	–	–	1	3	–	–	–	–	–	–	–	–
Damaliscus pygargus	Bontebok/Blesbok	–	–	1	1	1	1	1	2	–	–	–	–	1	1
Tragelaphus oryx	Eland	–	–	–	–	–	–	–	–	–	–	1	1	1	4
cf. Syncerus antiquus	Giant buffalo	–	–	–	–	1	1	–	–	–	–	–	–	–	–
	Bovid 1	2	9	1	1	2	18	2	15	3	62	2	7	1	4
	Bovid 1/2	–	–	–	–	–	–	–	–	–	–	–	–	1	1
	Bovid 2	3	13	1	4	3	42	2	31	3	30	1	14	2	40
	Bovid 2/3	–	–	–	–	1	2	1	7	1	3	–	–	1	4
	Bovid 3	1	6	2	10	3	20	2	29	2	45	1	2	1	40
	Bovid 3/4	–	–	–	–	2	7	–	–	1	7	1	1	1	6
	Bovid 4	1	1	1	2	1	3	–	–	1	4	1	3	1	19
	Large mammal	2	5	1	3	2	25	3	45	2	23	2	6	1	7
	Very large mammal	–	–	–	–	1	1	–	–	–	–	–	–	–	–
Total		25	192	21	81	41	397	40	423	38	646	21	180	25	230

PAY and PAZ are dominated by micromammal remains, and small mammals such as hyrax and Cape dune molerat with a few identified bovid bones. Lagomorph remains were recovered from PAY, PBC, PBD and PCA with one specimen identified as scrub hare (*Lepus saxatilis*). Equids (*Equus* sp.) are common in layers PBA/PBB and PBC and many of the 'large mammal' rib and vertebral fragments in these layers are probably equid remains. Based on variation in long bone and metapodia sizes, it is likely that the quagga (*Equus quagga quagga*) or plains zebra (*Equus quagga burchellii*) and mountain zebra (*Equus zebra*) may be present but the fragmented nature of the bones prevents positive identification. It is unclear whether the Cape zebra (*Equus capensis*) is present.

Cape grysbok or steenbok (*Raphicerus* sp.) occur in most layers and are most common in PBC, PBD and PBE. A single oribi (*Ourebia ourebia*) phalange was identified in PBA/PBB with sufficient morphological traits to distinguish this specimen from grey duiker (*Sylvicapra grimmia*), klipspringer (*Oreotragus oreotragus*) or the more common *Raphicerus*. Larger bovids are relatively more common in PBA/PBB, PBC and PCA. Blesbok or bontebok (*Damaliscus pygargus*) remains were recovered from these layers. One *Damaliscus* tooth fragment was noticeably larger than *D. pygargus* but smaller than tsessebe (*Damaliscus lunatus*) and may be the extinct blesbok (*Damaliscus niro*). Reedbuck (*Redunca* sp.) occurs in PBA/PBB and PBD. The vertebral fragment assigned to 'very large mammal' likely belongs to long-horned buffalo. Regarding alcelaphines, hartebeest was distinguishable from black wildebeest (*Connochaetes gnou*) by tooth morphology. For example, enamel infolds, particularly on the mesial region of the buccal surfaces of molars, are more pronounced in hartebeest than wildebeest. The relatively high number of 'large mammal' rib and vertebral specimens in layers PBA/PBB and PBC is probably related to the alcelaphines recovered from those layers. Eland remains are relatively more common in PCA and suggest that the other unidentified size 4 bovid specimens from that layer are also most likely eland since no African buffalo have been identified.

5.1.3. Comparisons with other sites

As is the case at KDS, small mammals (particularly dune molerat and hyrax), small bovids and tortoise are common in the pre-70 ka MSA layers at Blombos (Henshilwood et al., 2001; Thompson and

Henshilwood, 2014), in the HP layers at Diepkloof (Steele and Klein, 2013) and at Die Kelders (Klein and Cruz-Uribe, 2000). Of the large bovids recovered, eland is relatively common at Blombos, Die Kelders and Diepkloof but rare at KDS. In contrast, equid, quite common at Diepkloof and KDS, is only present in the earlier (~100 ka) M3 phase at Blombos and rare at Die Kelders. The prevalence of equids at KDS and within the HP layers at Diepkloof suggests a grassier environment during this period. *Damaliscus* does not occur at either Diepkloof or Blombos but is present at Die Kelders and KDS. While African buffalo occur at Blombos and Die Kelders, remains have not been recovered from KDS. Future studies of KDS fauna will include assessment of skeletal profiles and surface modification patterns.

5.2. Shellfish

The shellfish data presented are a sample of the material retained in the 3 mm sieve from a number of quadrates (between four and six per layer) spanning the sequence from PCA to PAY. This data represents 32.4% of the total volume excavated from these layers. Just over 29 kg of shellfish has been analysed from a volume of 0.51 m^3 and 7 layers. Shells were weighed and quantified by determining the minimum number of individuals (MNI) per layer, based on counting the apices of gastropods, the left and right umbos of bivalves with the most common side taken as the MNI, and the highest number of either front, back or middle valves (middle valve counts were divided by 6) of chitons was taken as the MNI. Both apices and opercula of the giant periwinkle *Turbo sarmaticus* were counted and the highest count taken as the MNI. The greatest dimensions of intact limpets and opercula were measured with digital callipers to the nearest millimetre. Shells that were <2 cm (whole) were not considered to be food items and were recorded as incidental shells or juvenile limpets.

In total, excluding the incidental and juvenile shells, 14 species of shellfish were identified (Table 8). Note that although two periwinkle species, *Diloma sinensis* and *Diloma tigrina*, are present, their data have been combined as the countable apices are not identifiable to species level when the shells are broken. Overall, the most common species, in terms of MNI (absolute, per m^3 and in terms of relative frequency), is the giant chiton, *Dinoplax gigas*, followed by the brown mussel, *Perna perna*, and *T. sarmaticus*. By weight, the most common species is the abalone, *Haliotis midae*, followed by *D. gigas*, and *T. sarmaticus*.

H. midae, *D. gigas* and *T. sarmaticus* are consistently the most common by weight relative to other species within layers, although frequencies differ between layers. As they are all relatively large animals with heavy shells, their dominance by weight is not that surprising, although they tend to dominate the assemblage in terms of MNI as well. Only in PAY is the Argenville's limpet, *Scutellastra argenvillei*, which is rare or absent in other layers, the second most common in terms of weight (38%). This could be a function of the smaller sample size in PAY. In terms of MNI, the range of the most common species is more varied between layers, but in most instances *D. gigas* and *T. sarmaticus* are most common, but the relative percentage of *P. perna* increases in most layers. Four species, the black mussel *Choromytilus meridionalis*, sand mussel *Donax serra*, kelp limpet *Cymbula compressa* and bearded limpet *Scutellastra barbara* are present in such small quantities that their contribution to the diet of the KDS occupants would have been minimal.

There is a shift in the relative percentage by weight of the three most common species – at the base of the sequence, PCA, *T. sarmaticus* is the most common, in PBE and PBD *H. midae* is the most common, in PBC *D. gigas* is only slightly more common than *H. midae*, and in all the layers above *D. gigas* is the most frequently occurring species by weight (Fig. 11). The same shift is evident from the density data (g/m^3) of these species.

5.2.1. Densities by layer

There is little or no shellfish present in layers below PCA. That which has been recorded is thought to derive from PCA above, where PCA and PCB could not be separated. Densities are considerably higher in layers PBC and PBD, with 183 kg/m^3 and 181 kg/m^3 respectively, than in any other layers (Table 8), and gradually decreases towards the top of the sequence, with less than 3 kg/m^3 in PAY. Shellfish volumes decrease drastically above PAY (<1 kg/m^3), and only increase again in layers PAQ (1.4 kg/m^3) and above (up to 12.2 kg/m^3 in PAL). Notwithstanding the effects of volume reduction over time and geomorphological processes that cannot be accounted for, PBC and PBD are very dense shell layers, both relative to other layers within this site, as well as to other MSA sites with shellfish remains and published volumes. At Klasies River, the highest recorded density of shellfish is in the MSA II, at 162 kg/m^3 (Thackeray, 1988). The HP layers at Klasies River show a gradual decline in shellfish volumes through time, starting at 8.7 kg/m^3 in the lower layers, and ending in 0.8 kg/m^3 in the uppermost HP layers. At Blombos, shellfish volumes are highest in layer CI in the M3 phase, c. 100 ka, at 163.8 kg/m^3 (Henshilwood et al., 2001), and lower in the M2 (c. 80 ka) and M1 (c. 75 ka, Still Bay) phases, with 31.8 kg/m^3 and 17.5 kg/m^3 respectively. At Pinnacle Point Cave PP13B, in layers dating between 90 and 164 ka, shell densities are relatively low, ranging from 0.01 kg/m^3 to 8.7 kg/m^3 (Jerardino and Marean, 2010). Shellfish data have not been provided for the HP layers at Pinnacle Point Site PP5–6, but densities appear to be low (Brown et al., 2012).

Although the density of shellfish declines with time, the species composition does not indicate a change in the distance from the shore significant enough to result in changes in collection strategies, for example an increase in *P. perna*, which can be transported over greater distances, or a decrease in large high yield species when distances exceed 5 km (Langejans et al., 2012).

5.2.2. Shellfish size

It has been argued that reductions in shellfish size can be used as a proxy for intensification of shellfish gathering and increased group size (e.g. Klein and Steele, 2013), although some suggest that the role of environmental factors on shellfish growth rates might be more significant than previously considered (Sealy and Galimberti, 2011). The number of measurable shells from the current sample is small, but has been included here for completeness. Very few of the *Cymbula granatina* shells were intact enough for measurement, and all are from PBD and PBC. From the small measurable sample ($n = 10$), the median is 67.5 mm, mean 67.4 mm, minimum 57 mm and maximum 79 mm. These sizes are smaller than the average of modern *C. granatina* from unexploited areas on the Cape west coast (Parkington et al., 2013), and somewhat smaller than those reported from MSA contexts on the west coast, except for Boegoeberg 2, where sizes are similar (Steele and Klein, 2008; exact measurements are not provided).

The current measurable *Cymbula oculus* sample is also small (median 72.5 mm, mean 71.2 mm, minimum 55 mm, maximum 84 mm, $n = 16$). These sizes are somewhat smaller than that of *C. oculus* from the HP at Klasies River, but bigger than any published LSA data (Klein and Steele, 2013).

All measurements ($n = 63$) of *T. sarmaticus* opercula are from layers PCA to PBA/PBB. The median length is 38 mm, mean 36.9 mm, minimum 14 mm and maximum 50 mm. This is smaller than those from the HP at Klasies River, larger than any published LSA opercula sizes, and most similar in size to those from the MSA I and II from Klasies River (Klein and Steele, 2013).

Table 8
Minimum number of individuals (MNI), weight (g) and density (MNI/m^3 and kg/m^3) of shellfish from layers PCA to PAY.

Species	PAY		PAZ		PBA/PBB		PBC		PBD		PBE		PCA	
	MNI	g	MNI	g	MNI	g	MNI	g	MNI	g	MNI	g	MNI	g
Choromytilus meridionalis	–	–	1	<1	–	–	1	<1	–	–	–	–	–	–
Perna perna	1	5	8	26	14	49	68	123	22	54	32	59	18	23
Donax serra	1	1	–	–	–	–	–	–	–	–	–	–	–	–
Burnupena cincta	2	2	2	10	4	94	56	323	8	46	4	9	1	4
Haliotis midae	1	2	1	47	2	334	18	3445	27	5739	12	2052	1	284
Cymbula compressa	–	–	1	3	1	2	1	3	1	20	2	5	–	–
Cymbula granatina	1	1	1	3	1	26	20	417	8	328	1	63	1	43
Cymbula oculus	1	1	1	10	13	119	16	220	21	380	10	210	5	59
Scutellastra argenvillei	1	48	1	3	1	<1	1	1	1	59	1	3	1	42
Scutellastra barbara	–	–	–	–	–	–	–	–	–	–	1	5	1	1
Patella spp.	–	3	1	12	–	29	–	36	–	65	–	49	–	89
Diloma sp.	–	–	1	5	1	24	17	54	3	3	6	3	1	30
Turbo sarmaticus	1	13	3	165	17	572	19	707	25	1265	30	1263	45	1290
Dinoplax gigas	6	54	25	742	114	1877	206	3612	25	1193	27	546	6	233
Shell fragments	–	7	–	19	–	155	–	121	–	47	–	54	–	19
Total MNI and g	15	135	46	1046	168	3281	423	9061	141	9197	126	4322	80	2118
Density MNI/m^3 and kg/m^3	294	3	703	16	1660	32	8526	183	2771	181	1159	40	931	25
Non-food species	-	–	–	–	–	–	–	–	–	–	–	–	–	–
Incidental shells	–	2	–	1	–	1	–	5	–	3	–	14	–	31
Juvenile *Patella* sp.	–	–	–	0	–	3	–	8	–	7	–	5	–	1

5.2.3. Collection strategies

The abundance of *D. gigas*, *H. midae* and *T. sarmaticus* indicates that the inhabitants were targeting species with high meat yield rates (Langejans et al., 2012). These three species contributed the highest average meat weight per m^3 in every layer (cf. Avery, 1976). They are usually only collectible at low tides and in the instance of *H. midae*, the kelp limpet *C. compressa* and *S. barbara*, spring low tides. Thus it appears that the majority of shellfish collection was scheduled to coincide with low tides.

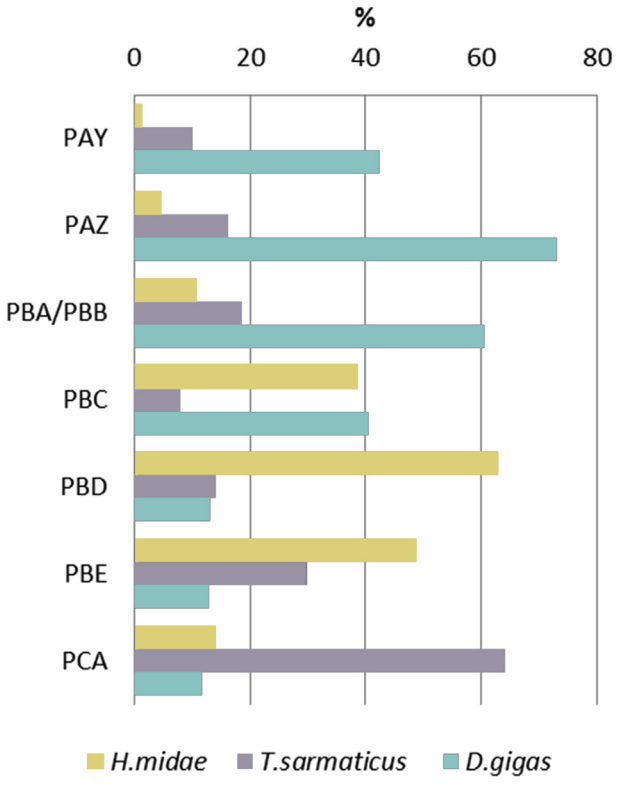

Fig. 11. Relative frequency (%) per layer of the three most common shellfish species based on weight.

5.3. Human remains

A nearly complete crown of an isolated human left mandibular deciduous second molar (Ldm2) was recovered from quadrate S29b, layer PBE dated at c. 64 ka (Fig. 4, PBE lies between layers dated to 64.6 ± 4.2 and 63.5 ± 4.7 ka). A description of the molar is in preparation by Havarti et al.

6. Palaeoenvironment

6.1. Fauna

The high densities of shellfish at KDS suggest that it was located close to the shore during most of the HP occupation. The cold water endemic shellfish species, *C. granatina*, or granite limpet, which does not occur on the south coast today, is present in relatively small quantities throughout the sequence, and most common in terms of weight (8.4 kg/m^3) in PBC. Their presence suggests that sea surface temperatures (SST) were cooler than present, although the abundant presence of warmer water species such as *T. sarmaticus* and *D. gigas* mitigates against extreme differences in temperature. The few fragments of *C. meridionalis*, a species most abundant on the colder west coast today, could also support cooler conditions, although it is probably only a good indicator of cooler conditions when it outnumbers its warmer water counterpart, *P. perna*, which is not the case here.

The species composition indicates rocky shores, with the exception of a few fragments of *D. serra* in PAY, which is a sandy beach inhabitant. The steady increase in *D. gigas* at the expense of *H. midae* and *T. sarmaticus* in the upper layers could indicate an increase in sandy conditions, as *D. gigas* is more tolerant of sandy environments than the other two species (Kilburn and Rippey, 1982; Wood, 1993; Yssel, 1989).

The terrestrial fauna from KDS consists largely of species that occurred in the area historically (Skead, 1980). The abundance of rock hyraxes indicates rocky hillsides associated with shrubs, consistent with the fynbos and rocky crevices surrounding KDS today. The presence of terrapin and reedbuck implies a nearby fresh-water source such as a wetland or riverbed. Southern reedbuck (*R. arundinum*) prefer tall grass or reed beds for cover and are typically found in grasslands adjacent to wetlands or *vleis*.

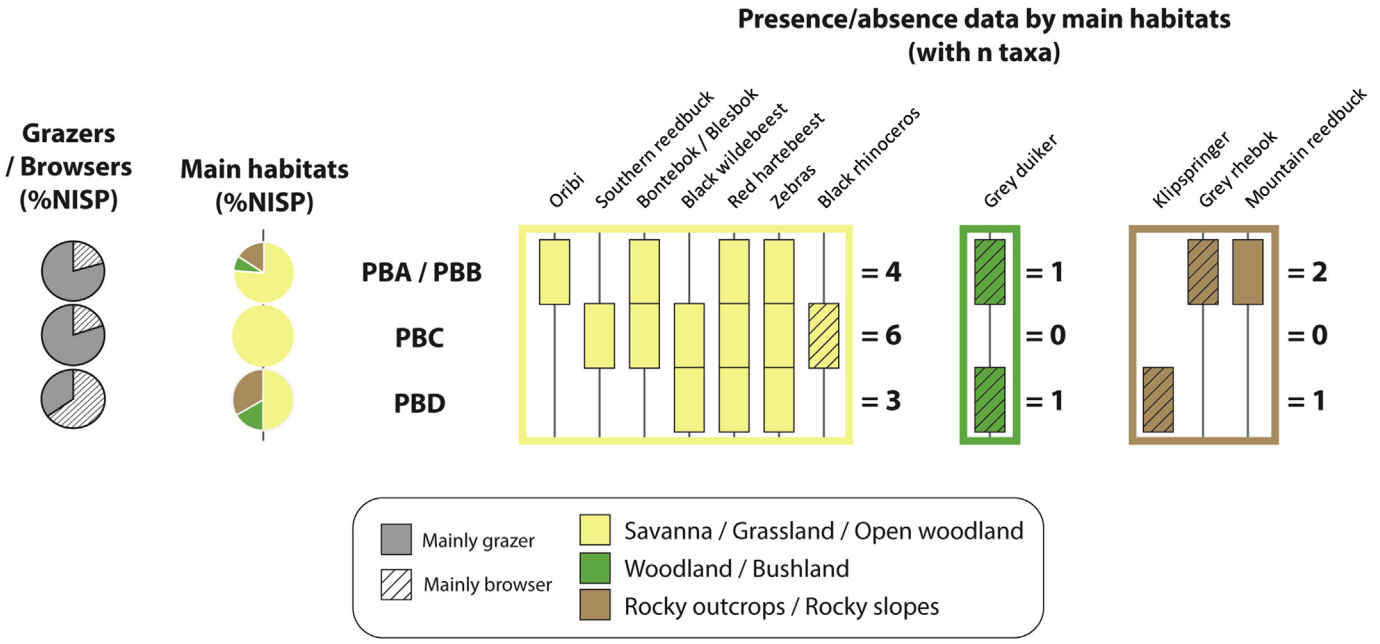

Fig. 12. Palaeoenvironmental analyses of large herbivore communities (grazer/browser ratios and data on main habitat preferences expressed as NISP proportions and presence/absence of each taxa).

Mountain reedbuck favour dry, grass-covered mountain slopes but also require the availability of fresh water (Skinner and Chimimba, 2005). The Klipdriftfontein stream lies close to KDS and could have been the source of this fresh water. Southern reedbuck is not known to occur in fynbos historically and its presence could indicate moister than present or historical conditions (Skead, 1980).

The presence of dune mole-rats in PAZ and PAY and the absence of this species in all other layers could indicate a change in the local environment to more sandy conditions. Dune molerats are associated with mesic coastal, sandy, environments (Bennett et al., 2009). Increase in size is thought to correlate with increased moisture (Klein, 1991). Unfortunately mole-rat remains from KDS were too fragmented for measurement. The lack of dune mole-rat remains in other layers may also be due to the small sample size or changes in taphonomic conditions across the sequence that have yet to be identified. Likewise the absence of Cape fur seal at KDS could be due to taphonomic and preservational issues, or the relatively small sample size. Conversely, seals may have been butchered close to the shore with little osteological material transported back to the site.

Palaeoenvironmental analyses of large herbivore communities are still tentative for KDS, as identified remains are rare. The sample sizes for layers PCA, PBE, PAZ and PAY are too small (total NISP <10) to allow for a secure interpretation. We thus focus here on layers PBD (total NISP $= 20$), PBC (40) and PBA/PBB (29). Although evidence for temporal changes should be treated with caution due to the current small sample size, some observations can be made.

Some patterns are apparent when large mammal data is interpreted in terms of grazer/browser ratios and main habitat preferences (Fig. 12, interpretations based on modern data cf. Rector and Reed, 2010; Skinner and Chimimba, 2005; Sponheimer et al., 2003). While 65% of identified bones in PBD correspond to ungulates that are mainly browsers (steenbok/grysbok, grey duiker and klipspringer), the upper HP layers indicate a considerable increase in ungulates that are mainly grazers (equids, red hartebeest, southern reedbuck, mountain reedbuck, black wildebeest, bontebok/blesbok and oribi). In layers PBC and PBA/PBB they represent 80% and 79% of identified ungulates respectively (Fig. 12).

This sharp increase in presence of grazers is parallelled by data relating to main habitat preferences. There appears to be a change from slightly more bushy terrain in PBD to an environment dominated by grasslands in PBC, potentially interspersed with woodlands and shrubs (as indicated by the presence of black rhinoceros). PBC documents the development of a full suite of ungulates that are preferentially found in open grassland/savannah ecosystems (6 out of the 6 taxa identified in the layer), with equids representing 63% of identified ungulates. The environment in PBA/PBB is somewhat intermediate between PBD and PBC.

The development of a grassland-dominated ecosystem in PBC around 66 ka may correspond to an increased frequency of C4 plants following an increase in summer rain. Isotopic studies of the nearby Crevice Cave speleothems (Bar-Matthews et al., 2010) support this hypothesis: in these records, increases in $\delta^{13}C$ and $\delta^{18}O$ around 68 ka have been interpreted as indicative of correlated increases in C4 plants and in summer rain respectively.

7. Discussion

The comprehensive data collection strategy adopted at KDS during the 2011–2013 excavations of the HP layers, and the subsequent and on-going analysis of this assemblage, allows for preliminary observations to be made and provide a sound basis for future excavations at the site. The small assemblage recovered from the upper layers of KDS (PAL – PAN/PAO) with an age of 51.7 ± 3.3 ka provides a tentative glimpse of the post-HP layers and will be one focus of future excavations.

The HP layers at KDS have been dated by OSL to 65.5 ± 4.8 ka to 59.4 ± 4.6 ka. Similar OSL dates have been attained for a number of other HP assemblages in southern Africa, suggesting that the HP is a relatively short-lived industry (Jacobs et al., 2008). However, the chronology produced by Jacobs et al. (2008) has recently been questioned by Guérin et al. (2013), who claim that the HP ages are erroneously precise, and that the "adjusted dose rate" model used by Jacobs et al. (2008) is incorrect. It is beyond the scope of this paper to attempt to adjudicate either criticism, but we note that the

"adjusted dose rate" model was not applied to KDS samples, and individual ages presented here have relative uncertainties which are consistent with the expectations of Guérin et al. (2013). New OSL and thermoluminescence ages from Diepkloof (Tribolo et al., 2013) also contradict the findings of Jacobs et al. (2008), indicating a much longer HP chronology, with an early HP at c. 109 ka and a final HP at c. 52 ka. The full range of these latter ages for the HP is not evident at KDS.

The lithic assemblages from PCA to PAY correlate with the HP complex. They evidence a number of changes, involving raw material composition, frequencies and types of retouched tools, which relate to three main phases occurring during a gradual process of change. Similar patterns of change through time are documented at Klasies River (Villa et al., 2010; Wurz, 2000) and at Diepkloof in the intermediate and late HP layers (Porraz et al., 2013a, 2013b). The lower KDS layers (PCA, PBE) share a number of similarities with the lower phase at Klasies River and the Intermediate HP phase at Diepkloof, while the middle KDS layers (PBC, PBA/PBB) correspond to the upper part of the sequence at Klasies River and to the late HP at Diepkloof. This diagnosis for KDS is based on the layers which are currently available for analysis. Further research on the underlying and overlying layers will undoubtedly complete and refine this preliminary assessment.

In terms of ochre processing strategies and geological diversity, the KDS assemblage appears to exhibit four distinctive phases. Whereas the lowest layer (PCA) resembles PBD and PBC in terms of displaying the standard range of processing techniques and geological varieties, layer PBE consists of a dense concentration of thoroughly processed shale-derived red ochre. PBE contains the highest concentration of red ochre derived from fissile shales, and the range of geological types are limited relative to other layers in the sequence. Layer PBE therefore represents a break in standard pigment selection and processing strategies displayed by the samples recovered from layers PAY to PBD. As powdered ochre may have been used for various purposes (Bonneau et al., 2012, d'Errico et al., 2012; Henshilwood et al., 2009, 2011; Rifkin, 2011; Soriano et al., 2009; Wadley et al., 2009), such high volumes may be indicative of the deliberate processing of large amounts of ochre for very specific purposes. Following this emphasis on processing ochre into fine powder, layer PBC exhibits the largest assembly of ochre crayons and the widest geological variability. In layer PBA/PBB, the raw material composition remains largely unchanged but there is increased evidence for flaking as a primary processing strategy. The upper layers (PAY and PAZ) display the least variability in terms of raw material selection and processing technique employed.

The prevalence of small mammals and tortoise at KDS is similar to that found at many other MSA sites in the southern and western Cape. Larger mammal data from KDS – particularly alcelaphines and equids – suggests an environment where grasses feature more prominently than they did historically, as has been noted for the HP layers at Diepkloof (Steele and Klein, 2013). In other reports significant faunal changes during the HP period are not emphasized. At KDS, while most layers (PAZ, PBA/PBB, PBC and PCA) are dominated by remains of medium and large mammals (mainly bovids and equids), others are dominated by tortoise remains (PBD and PBE) and layer PAY by small mammals (particularly rock hyrax and Cape dune molerat). The KDS sequence also documents changes in the relative proportion of small bovids (e.g. Cape grysbok/steenbok, klipspringer, grey duiker; more common in layers such as PBD) and of equids and larger bovids (e.g. red hartebeest, black wildebeest, bontebok/blesbok, eland – more common in layers such as PBC). Further studies of the KDS fauna will include taphonomical analyses to decipher how these patterns correlate with environmental and/or subsistence changes. The significant extent of these faunal changes might imply that HP hunter-gatherers changed their subsistence strategies and adapted to varying environments, while not necessarily modifying the main characteristics of their technical and cultural behaviours. KDS can play a role in future research focused on understanding the interplay between cultural changes, especially in lithic technology (see 4.1 above), and subsistence strategies during the HP.

The shellfish data here complement that from other known HP locations with shellfish such as Klasies River and Diepkloof. As at Klasies River, the density of shellfish declines with time through the HP (Thackeray, 1988), whereas the opposite is true at Diepkloof (Steele and Klein, 2013). The high density of shellfish, particularly in layers PBC and PBD, suggests that the coastline was nearby, and lower densities in the younger layers could reflect a retreat of the coast due to lowering sea levels. Conversely, the presence of dune mole-rat remains only in the upper layers PAY and PAZ, where shellfish densities are lowest, implies the presence of dune sand and a nearby coastline. More data are needed to address these conflicting signals. The low incidence of fish bones could be due to taphonomic processes as bone is generally poorly preserved and fragmented, and fish bone is even more susceptible to degradation than mammalian bone (Szpak, 2011).

Ostrich eggshell is abundant throughout the site. The presence of at least 95 OES pieces engraved with abstract patterns, similar to that reported from only two other HP contexts, Diepkloof and Apollo 11, extends the geographic extent of this cultural tradition.

8. Conclusion

KDS is a newly discovered coastal site in the southern Cape containing lithics typical of the HP. It is the first known typical HP site (see Henshilwood, 2012) located on the c. 600 km of coastline between Nelson Bay Cave, Plettenberg Bay and Peers Cave (Skildegat) on the Cape Peninsula (Fig. 1). No anthropogenic deposits were recovered at KDS that predate 65.5 ± 4.8 suggesting that the c. 71 ka early HP-like technology reported at Pinnacle Point (Brown et al., 2012) and the >c. 72 ka Still Bay phases from nearby Blombos Cave (Henshilwood, 2012) are technocomplexes that predate the KDS HP deposits. Nevertheless, the KDS assemblage provides a useful corollary with the earlier Blombos and Pinnacle Point data on coastal subsistence patterns during the MSA in this region. Future excavations at the adjacent KDCL site with MSA deposits that predate c. 70 ka, and of the post –HP layers (for which a single age of 51.7 ± 3.3 ka is currently available) at KDS, will add to this knowledge. The apparent absence of shellfish at this site is worth noting.

The current faunal sample from KDS is too small for definitive statements regarding environmental conditions during the HP in this region, although tentatively, the macromammal and shellfish data point to some changes in rainfall regimes and local environments within the sequence. Additional data from microfauna, isotopic analysis and larger macrofaunal samples will contribute to refining these observations and to the greater picture of environmental conditions during this period. It is worth noting that the environmental change that is evident in layer PBC apparently corresponds to a change in lithic raw materials, from a predominant exploitation of silcrete to an increased importance of quartz exploitation and also a marked decrease in pigment exploitation. Future research on the KDS HP will focus on understanding the role played by environmental changes in the evolution of raw material and food procurement strategies by MSA hunter-gatherers. The development of an open landscape might have influenced general mobility strategies, affecting both hunted species and access to raw materials.

Whether the engraved OES from KDS indicates continuity in the practice of marking or decoration of material culture in the

southern Cape, as is evidenced at Blombos (Henshilwood et al., 2009) in the Still Bay and pre-Still Bay layers, is not clear at this stage. This is especially so as there is an anthropogenically sterile sand layer above the terminal MSA deposits at Blombos and below the first MSA deposits at KDS. However, the planned detailed studies of the KDS engraved OES may provide further evidence on likely cultural links with other Western Cape sites.

The recent discovery and excavation of KDS helps reinforce the notion that *H. sapiens* using HP technology were fairly widely spread in South Africa between 66 and 59 ka, were able to adapt to a range of environmental conditions and yet produced a technology that is fairly standardized. The latter suggests a deliberate continuity in material culture styles probably reinforced by frequent contact among and between the groups that ranged across this region. Some of the cultural traditions, such as the engraving of OES, appear infrequently, but their presence in sites on the west coast and now the southern Cape reinforces this notion of contact within a far reaching social network.

Acknowledgements

Financial support for the KDS project was provided to CSH by a European Research Council Advanced Grant, TRACSYMBOLS No. 249587, awarded under the FP7 programme at the University of Bergen, Norway and by a National Research Foundation/Department of Science and Technology funded Chair at the University of the Witwatersrand, South Africa. Additional funding for the KDS excavations in 2013 was provided by the National Geographic Expeditions Council, grant number EC0592-12. We would like to extend thanks to the board of Cape Nature, and especially Tierck Hoekstra and Callum Beattie, for access to the Klipdrift Complex and the facilities at Potberg. We thank Kurt Muchler at NGS, and John Compton for useful comments. We thank Gauthier Devilder for the lithic drawings. Shaw Badenhorst at the Ditsong National Museum of Natural History provided help in the mammalian faunal identification and allowed access to their faunal reference collection. We thank the anonymous referees for their helpful and constructive suggestions.

References

Armitage, S.J., Bailey, R.M., 2005. The measured dependence of laboratory beta dose rates on sample grain size. Radiat. Meas. 39, 123–127.
Armitage, S.J., King, G.E., 2013. Optically stimulated luminescence dating of hearths from the Fazzan Basin, Libya: a tool for determining the timing and pattern of Holocene occupation of the Sahara. Quat. Geochronol. 15, 88–97. http://dx.doi.org/10.1016/j.quageo.2012.10.002.
Armitage, S.J., Jasim, S.A., Marks, A.E., Parker, A.G., Usik, V.I., Uerpmann, H.-P., 2011. The southern route out of Africa: evidence for an early expansion of modern humans into Arabia. Science 331, 453–456. http://dx.doi.org/10.1126/science.1199113.
Avery, G., 1976. A Systematic Investigation of Open Station Shell Middens along the Southwestern Cape Coast. University of Cape Town.
Bar-Matthews, M., Marean, C.W., Jacobs, Z., Karkanas, P., Fisher, E.C., Herries, A.I., Brown, K., Williams, H.M., Bernatchez, J., Ayalon, A., 2010. A high resolution and continuous isotopic speleothem record of paleoclimate and paleoenvironment from 90 to 53 ka from Pinnacle Point on the south coast of South Africa. Quat. Sci. Rev. 29, 2131–2145. http://dx.doi.org/10.1016/j.quascirev.2010.05.009.
Bateman, M.D., Holmes, P.J., Carr, A.S., Horton, B.P., Jaiswal, M.K., 2004. Aeolianite and barrier dune construction spanning the last two glacial-interglacial cycles from the southern Cape coast, South Africa. Quat. Sci. Rev. 23, 1681–1698. http://dx.doi.org/10.1016/S0277-3791(04)00043-5.
Bennett, N.C., Faulkes, C.G., Hart, L., Jarvis, J.U.M., 2009. *Bathyergus suillus* (Rodentia: Bathyergidae). Mamm. Species 828, 1–7. http://dx.doi.org/10.1644/828.1.
Bonneau, A., Pearce, D., Pollard, A., 2012. A multi-technique characterization and provenance study of the pigments used in San rock art, South Africa. J. Archaeol. Sci. 39, 287–294. http://dx.doi.org/10.1016/j.jas.2011.09.011.
Bøtter-Jensen, L., Andersen, C.E., Duller, G.A.T., Murray, A.S., 2003. Developments in radiation, stimulation and observation facilities in luminescence measurements. Radiat. Meas. 37, 535–541.
Brain, C.K., 1974. Some suggested procedures in the analysis of bone accumulations from southern African Quaternary sites. Ann. Transvaal Mus. 29, 1–8.
Brown, K.S., Marean, C.W., Jacobs, Z., Schoville, B.J., Oestmo, S., Fisher, E.C., Bernatchez, J., Karkanas, P., Matthews, T., 2012. An early and enduring advanced technology originating 71,000 years ago in South Africa. Nature 491, 590–593.
Carr, A., Bateman, M., Holmes, P., 2007. Developing a 150 ka luminescence chronology for the barrier dunes of the southern Cape, South Africa. Quat. Geochronol. 2, 110–116.
Chapot, M.S., Roberts, H.M., Duller, G.A.T., Lai, Z.P., 2012. A comparison of natural- and laboratory-generated dose response curves for quartz optically stimulated luminescence signals from Chinese Loess. Radiat. Meas. 47, 1045–1052.
Compton, J.S., 2001. Holocene sea-level fluctuations inferred from the evolution of depositional environments of the southern Langebaan Lagoon salt marsh, South Africa. Holocene 11, 395–405.
Compton, J.S., 2011. Pleistocene sea-level fluctuations and human evolution on the southern coastal plain of South Africa. Quat. Sci. Rev. 30, 506–527.
Conard, N., Porraz, G., Wadley, L., 2012. What is in a name? Characterizing the "post-Howieson's Poort" at Sibudu. S. Afr. Archaeol. Bull. 67, 180–199.
Cornell, R.M., Schwertmann, U., 2003. The Iron Oxides: Structure, Properties, Reactions, Occurrences and Uses. Wiley, Weinheim.
Dayet, L., Texier, P.-J., Daniel, F., Porraz, G., 2013. Ochre resources from the Middle Stone Age sequence of Diepkloof Rock Shelter, Western Cape, South Africa. J. Archaeol. Sci. 40, 3492–3505.
Deacon, H.J., Geleijnse, V.B., 1988. The stratigraphy and sedimentology of the main site sequence, Klasies River, South Africa. S. Afr. Archaeol. Bull. 43, 5–14.
Driver, J.C., 2005. Manual for Description of Vertebrae Remains. Crow Canyon Archaeological Center, Cortez. http://dx.doi.org/10.6067/XCV8BP01K6.
Duller, G.A.T., Bøtter-Jensen, L., Murray, A.S., Truscott, A.J., 1999. Single grain laser luminescence (SGLL) measurements using a novel automated reader. Nucl. Instrum. Methods Phys. Res. Sect. B: Beam Interact. Mater. Atoms 155, 506–514. http://dx.doi.org/10.1016/S0168-583X(99)00488-7.
Duller, G.A.T., Bøtter-Jensen, L., Murray, A.S., 2000. Optical dating of single sand-sized grains of quartz: sources of variability. Radiat. Meas. 32, 453–457.
d'Errico, F., García Moreno, R., Rifkin, R.F., 2012. Technological, elemental and colorimetric analysis of an engraved ochre fragment from the Middle Stone Age levels of Klasies River Cave 1. S. Afr. J. Archaeol. Sci. 39, 942–952.
Eastaugh, N., Walsh, V., Chaplin, T., Siddall, R., 2008. Pigment Compendium: a Dictionary and Optical Microscopy of Historic Pigments. Butterworth Heinemann, Oxford.
Essop, M.F., Harley, E.H., Baumgarten, I., 1997. A molecular phylogeny of some bovidae based on restrictive-site mapping of mitochondrial DNA. J. Mammal. 78, 377–386.
Faith, J.T., 2013. Taphonomic and paleoecological change in the large mammal sequence from Boomplaas Cave, western Cape, South Africa. J. Hum. Evol. 65 (6), 715–730.
Galbraith, R.F., Roberts, R.G., Laslett, G.M., Yoshida, H., Olley, J.M., 1999. Optical dating of single and multiple grains of quartz from Jinmium rock shelter, Northern Australia: part 1, experimental design and statistical models. Archaeometry 41, 339–364.
Gentry, A.W., 2010. Bovidae. In: Werdelin, L., Sanders, W.J. (Eds.), Cenozoic Mammals of Africa. University of California Press, Berkeley, pp. 741–796.
Guérin, G., Murray, A.S., Jain, M., Thomsen, K.J., Mercier, N., 2013. How confident are we in the chronology of the transition between Howieson's Poort and Still Bay. J. Hum. Evol. 64 (4), 314–317.
Henshilwood, C.S., 2012. Late Pleistocene Techno-traditions in Southern Africa: a review of the Still Bay and Howiesons Poort, c. 75–59 ka. J. World Prehist. 25, 205–237. http://dx.doi.org/10.1007/s10963-012-9060-3.
Henshilwood, C.S., Sealy, J.C., Yates, R., Cruz-Uribe, K., Goldberg, P., Grine, F.E., Klein, R.G., Poggenpoel, C.A., van Niekerk, K., Watts, I., 2001. Blombos Cave, Southern Cape, South Africa: preliminary report on the 1992-1999 excavations of the Middle Stone Age levels. J. Archaeol. Sci. 28, 421–448.
Henshilwood, C.S., d'Errico, F., Watts, I., 2009. Engraved ochres from the Middle Stone Age levels at Blombos Cave, South Africa. J. Hum. Evol. 57, 27–47. http://dx.doi.org/10.1016/j.jhevol.2009.01.005.
Henshilwood, C.S., d'Errico, F., van Niekerk, K.L., Coquinot, Y., Jacobs, Z., Lauritzen, S.-E., Menu, M., García-Moreno, R., 2011. A 100,000-year-old ochre-processing workshop at Blombos Cave, South Africa. Science 334, 219–222. http://dx.doi.org/10.1126/science.1211535.
Hodgskiss, T., 2010. Identifying grinding, scoring and rubbing use-wear on experimental ochre pieces. J. Archaeol. Sci. 37, 3344–3358.
http://tracsymbols.eu, 20/01/2014.
http://www.ncscolour.com, 2013.
Igreja, M., Porraz, G., 2013. Functional insights into the innovative Early Howiesons Poort technology at Diepkloof Rock Shelter (Western Cape, South Africa). J. Archaeol. Sci. 40, 3475–3491. http://dx.doi.org/10.1016/j.jas.2013.02.026.
Jacobs, Z., Roberts, R.G., 2007. Advances in optically stimulated luminescence dating of individual grains of quartz from archeological deposits. Evol. Anthropol. Issues News Rev. 16, 210–223.
Jacobs, Z., Roberts, R.G., Galbraith, R.F., Deacon, H.J., Grun, R., Mackay, A., Mitchell, P., Vogelsang, R., Wadley, L., 2008. Ages for the Middle Stone Age of Southern Africa: implications for human behavior and dispersal. Science 322, 733–735.
Jerardino, A., Marean, C.W., 2010. Shellfish gathering, marine paleoecology and modern human behavior: perspectives from cave PP13B, Pinnacle Point, South Africa. J. Hum. Evol. 59, 412–424.
Kilburn, R., Rippey, E., 1982. Sea Shells of Southern Africa. MacMillan South Africa, Johannesburg.

Klein, R.G., 1991. Size variation in the Cape dune molerat (*Bathyergus suillus*) and Late Quaternary climatic change in the southwestern Cape Province, South Africa. Quat. Res. 36, 243–256.
Klein, R.G., Cruz-Uribe, K., 1984. The Analysis of Animal Bones from Archaeological Sites. University of Chicago Press, Chicago.
Klein, R.G., Cruz-Uribe, K., 2000. Middle and Later Stone Age large mammal and tortoise remains from Die Kelders Cave 1, Western Cape Province, South Africa. J. Hum. Evol. 38, 169–195.
Klein, R.G., Steele, T.E., 2013. Archaeological shellfish size and later human evolution in Africa. Proc. Natl. Acad. Sci. U. S. A. 110, 10910–10915. http://dx.doi.org/10.1073/pnas.1304750110.
Langejans, G.H., van Niekerk, K.L., Dusseldorp, G.L., Thackeray, J.F., 2012. Middle Stone Age shellfish exploitation: potential indications for mass collecting and resource intensification at Blombos Cave and Klasies River, South Africa. Quat. Int. 270, 80–94. http://dx.doi.org/10.1016/j.quaint.2011.09.003.
Lombard, M., Wadley, L., Deacon, J., Wurz, S., Parsons, I., Mohapi, M., Swart, J., Mitchell, P., 2012. South African and Lesotho Stone Age sequence updated (I). S. Afr. Archaeol. Bull. 67, 120–144.
Low, A.B., Rebelo, A.G., 1996. Vegetation of South Africa, Lesotho and Swaziland. Department of Environmental Affairs & Tourism, Pretoria.
Malan, J., 1990. The Stratigraphy and Sedimentology of the Bredasdorp Group, Southern Cape Province. University of Cape Town.
Marker, M.E., Craven, S.A., 2002. The karst of the De Hoop Nature Reserve, Western Cape, South Africa. Cave Karst Sci. 29, 51–56.
Marshall, F., Pilgram, T., 1993. NISP vs. MNI in quantification of body-part representation. Am. Antiq. 58, 261–269.
Murray, A.S., Olley, J.M., 2002. Precision and accuracy in the optically stimulated luminescence dating of sedimentary quartz: a status review. Geochronometrica 21, 1–16.
Murray, A.S., Wintle, A.G., 2000. Luminescence dating of quartz using an improved single-aliquot regenerative-dose protocol. Radiat. Meas. 32, 57–73.
Olley, J.M., De Deckker, P., Roberts, R.G., Fifield, L.K., Yoshida, H., Hancock, G., 2004. Optical dating of deep-sea sediments using single grains of quartz: a comparison with radiocarbon. Sediment. Geol. 169, 175–189.
Parkington, J., Fisher, J.W., Kyriacou, K., 2013. Limpet gathering strategies in the Later Stone Age along the Cape West Coast, South Africa. J. Isl. Coast. Archaeol. 8, 91–107. http://dx.doi.org/10.1080/15564894.2012.756084.
Pickering, R., Jacobs, Z., Herries, A.I., Karkanas, P., Bar-Matthews, M., Woodhead, J.D., Kappen, P., Fisher, E., Marean, C.W., 2013. Paleoanthropologically significant South African sea caves dated to 1.1–1.0 million years using a combination of U–Pb, TT-OSL and palaeomagnetism. Quat. Sci. Rev. 65, 39–52.
Porraz, G., Parkington, J.E., Rigaud, J.-P., Miller, C.E., Poggenpoel, C., Tribolo, C., Archer, W., Cartwright, C.R., Charrié-Duhaut, A., Dayet, L., Igreja, M., Mercier, N., Schmidt, P., Verna, C., Texier, P.-J., 2013a. The MSA sequence of Diepkloof and the history of southern African Late Pleistocene populations. J. Archaeol. Sci. 40, 3542–3552. http://dx.doi.org/10.1016/j.jas.2013.02.024.
Porraz, G., Texier, P.-J., Archer, W., Piboule, M., Rigaud, J.-P., Tribolo, C., 2013b. Technological successions in the Middle Stone Age sequence of Diepkloof Rock Shelter, Western Cape, South Africa. J. Archaeol. Sci. 40, 3376–3400. http://dx.doi.org/10.1016/j.jas.2013.02.012.
Prescott, J.R., Hutton, J.T., 1994. Cosmic ray contributions to dose rates for luminescence and ESR dating: large depths and long-term time variations. Radiat. Meas. 23, 497–500.
Rector, A.L., Reed, K.E., 2010. Middle and late Pleistocene faunas of Pinnacle Point and their paleoecological implications. J. Hum. Evol. 59, 340–357.
Rifkin, R.F., 2011. Assessing the efficacy of red ochre as a prehistoric hide tanning ingredient. J. Afr. Archaeol. 9, 131–158.
Roberts, D.L., 2003. Age, Genesis and Significance of South African Coastal Belt Silcretes. Council for Geoscience, Pretoria.
Roberts, R.G., Galbraith, R.F., Olley, J.M., Yoshida, H., Laslett, G.M., 1999. Optical dating of single and multiple grains of quartz from Jinmium Rock Shelter, northern Australia: part II, results and implications. Archaeometry 41, 365–395. http://dx.doi.org/10.1111/j.1475-4754.1999.tb00988.x.
Roberts, R.G., Galbraith, R.F., Yoshida, H., Laslett, G.M., Olley, J.M., 2000. Distinguishing dose populations in sediment mixtures: a test of single-grain optical dating procedures using mixtures of laboratory-dosed quartz. Radiat. Meas. 32, 459–465.
Roberts, D.L., Botha, G.A., Maud, R.R., Pether, J., 2006. Coastal cenozoic deposits. In: Johnson, M.R., Anhaeusser, C.R., Thomas, R.J. (Eds.), The Geology of South Africa. Council for Geoscience, Pretoria, Geological Society of South Africa, Johannesburg, pp. 605–628.
Rogers, J., 1988. Stratigraphy and geomorphology of three generations of regressive sequences in the Bredasdorp Group, Southern Cape Province, South Africa. In: Dardis, G.F., Moon, B.P. (Eds.), Geomorphological Studies in Southern Africa. A.A. Balkema, Rotterdam, pp. 407–433.
Scott, H.A., Burgers, C.J., 1993. A Preliminary Inventory of Sensitive Habitats in the De Hoop Nature Reserve. Cape Nature Conservation, Cape Town.
Sealy, J., Galimberti, M., 2011. Shellfishing and the interpretation of shellfish sizes in the Middle and Later Stone Ages of South Africa. In: Bicho, N.F., Haws, J.A., Davis, L.G. (Eds.), Trekking the Shore. Springer, New York, pp. 405–419.
Skead, C.J., 1980. Historical mammal incidence in the Cape Province. Department of Nature and Environmental Conservation of the Provincial Administration of the Cape of Good Hope, Cape Town.
Skinner, J.D., Chimimba, C.T., 2005. The Mammals of the Southern African Subregion, third ed. Cambridge University Press, Cambridge.
Smith, M.A., Prescott, J.R., Head, M.J., 1997. Comparison of 14C and luminescence chronologies at Puritjarra rock shelter, central Australia. Quat. Sci. Rev. 16, 299–320.
Soriano, S., Villa, P., Wadley, L., 2007. Blade technology and tool forms in the Middle Stone Age of South Africa: the Howiesons Poort and post-Howiesons Poort at rose Cottage Cave. J. Archaeol. Sci. 34, 681–703.
Soriano, S., Villa, P., Wadley, L., 2009. Ochre for the toolmaker: shaping the Still Bay points at Sibudu (KwaZulu-Natal, South Africa). J. Afr. Archaeol. 7, 41–54.
Sponheimer, M., Lee-Thorp, J.A., DeRuiter, D.J., Smith, J.M., van der Merwe, N.J., Reed, K., Grant, C., Ayliffe, L.K., Robinson, T.F., Heidelberger, C., 2003. Diets of southern African Bovidae: stable isotope evidence. J. Mammal. 84, 471–479.
Steele, T.E., Klein, R.G., 2008. Intertidal shellfish use during the Middle and Later Stone Age of South Africa. Archaeofauna 17, 63–76.
Steele, T.E., Klein, R.G., 2013. The Middle and Later Stone Age faunal remains from Diepkloof Rock Shelter, Western Cape, South Africa. J. Archaeol. Sci. 40, 3453–3462.
Szpak, P., 2011. Fish bone chemistry and ultrastructure: implications for taphonomy and stable isotope analysis. J. Archaeol. Sci. 38, 3358–3372.
Texier, J.-P., Porraz, G., Parkington, J., Rigaud, J.-P., Poggenpoel, C., Miller, C., Tribolo, C., Cartwright, C., Coudenneau, A., Klein, R., Steele, T., Vernai, C., 2010. A Howiesons Poort tradition of engraving ostrich eggshell containers dated to 60,000 years ago at Diepkloof Rock Shelter, South Africa. Proc. Natl. Acad. Sci. U. S. A. 107 (14), 6180–6185.
Texier, P.-J., Porraz, G., Parkington, J., Rigaud, J.-P., Poggenpoel, C., Tribolo, C., 2013. The context, form and significance of the MSA engraved ostrich eggshell collection from Diepkloof Rock Shelter, Western Cape, South Africa. J. Archaeol. Sci. 40, 3412–3431. http://dx.doi.org/10.1016/j.jas.2013.02.021.
Thackeray, J.F., 1988. Molluscan fauna from Klasies River, South Africa. S. Afr. Archaeol. Bull. 43, 27–32.
Thompson, J.C., Henshilwood, C.S., 2014. Tortoise taphonomy and tortoise butchery patterns at Blombos Cave, South Africa. J. Archaeol. Sci. 41, 214–229.
Tribolo, C., Mercier, N., Douville, E., Joron, J.L., Reyss, J.L., Rufer, D., Cantin, N., Lefrais, Y., Miller, C.E., Porraz, G., Parkington, J., Rigaud, J.P., Texier, P.J., 2013. OSL and TL dating of the Middle Stone Age sequence at Diepkloof Rock Shelter (South Africa): a clarification. J. Archaeol. Sci. 40, 3401–3411. http://dx.doi.org/10.1016/j.jas.2012.12.001.
Van Andel, T.H., 1989. Late Pleistocene sea levels and the human exploitation of the shore and shelf of southern South Africa. J. Field Archaeol. 16, 133–154.
Villa, P., Delagnes, A., Wadley, L., 2005. A late Middle Stone Age artifact assemblage from Sibudu (KwaZulu-Natal): comparisons with the European Middle Paleolithic. J. Archaeol. Sci. 32, 399–422.
Villa, P., Soriano, S., Teyssandier, N., Wurz, S., 2010. The Howiesons Poort and MSA III at Klasies River main site, Cave 1A. J. Archaeol. Sci. 37, 630–655.
Vogelsang, R., Richter, J., Jacobs, Z., Eichhorn, B., Linseele, V., Roberts, R., 2010. New excavations of Middle Stone Age deposits at Apollo 11 rockshelter, Namibia: stratigraphy, archaeology, chronology and past environments. J. Afr. Archaeol. 8, 185–210.
Vorster, C.J., 2003. Simplified Geology: South Africa, Lesotho and Swaziland. Council for Geoscience, Pretoria.
Wadley, L., Hodgskiss, T., Grant, M., 2009. Implications for complex cognition from the hafting of tools with compound adhesives in the Middle Stone Age, South Africa. Proc. Natl. Acad. Sci. U. S. A. 106, 9590.
Watts, I., 2002. Ochre in the Middle Stone Age of Southern Africa: ritualised display or hide preservative? S. Afr. Archaeol. Bull. 57, 64–74.
Watts, I., 2009. Red ochre, body painting and language: interpreting the Blombos ochre. In: Botha, R., Knight, C. (Eds.), The Cradle of Language. Oxford University Press, Oxford, pp. 62–92.
Watts, I., 2010. The pigments from Pinnacle Point Cave 13B, Western Cape, South Africa. J. Hum. Evol. 59, 392–411. http://dx.doi.org/10.1016/j.jhevol.2010.07.006.
Willis, C.K., Cowling, R.M., Lombard, A.T., 1996. Patterns of endemism in the limestone flora of South African lowland fynbos. Biodivers. Conserv. 5, 55–73.
Wintle, A.G., Murray, A.S., 2006. A review of quartz optically stimulated luminescence characteristics and their relevance in single-aliquot regeneration dating protocols. Radiat. Meas. 41, 369–391.
Wood, A.D., 1993. Aspects of the Biology and Ecology of the South African abalone Haliotis midae Linnaeus, 1758 (Mollusca: Gastropoda) along the Eastern Cape and Ciskei Coast. Rhodes, p. 161.
Wurz, S., 2000. The Middle Stone Age at Klasies River. University of Stellenbosch, South Africa.
Yssel, S.G., 1989. Long-term Trends in a Population of Turbo sarmaticus, Linnaeus 1758, in the Tsitsikamma Coastal National Park. University of Port Elizabeth, p. 132.